Supporting Information

Iron(II) and Ruthenium(II) Complexes Containing P, N, and H Ligands: Structure, Spectroscopy, Electrochemistry and Reactivity

Jinzhu Chen, David J. Szalda, Etsuko Fujita, and Carol Creutz

Chemistry Department, Brookhaven National Laboratory, Upton, NY 11973-5000

[†]Department of Natural Sciences, Baruch College, New York, NY 10010, USA.

ccreutz@bnl.gov

Contents

Preparation and characterization of 7, 8, and 9.

[CpFe(CO)(bpy)]I. Synthesis of this compound in refluxing benzene was reported by Treichel et al., but only sparse ^{1}H NMR data (Cp 4.79 ppm) were reported.[1] A mixture of $[CpFe(CO)_2]I$ (200 mg, 0.66 mmol) and an equivalent quantity of bpy (103 mg, 0.66 mmol) in 100 mL of degassed toluene was exposed to ultraviolet irradiation (Englehard-Hanovia water-cooled 450-W mercury lamp) at room temperature for 4.0 hrs under nitrogen. The resulting red precipitate was filtered, washed with toluene and diethyl ether and dried under vacuum. Pure dark red crystals of [CpFe(CO)(bpy)]I (161 mg, yield 56%) were obtained by diffusion of diethyl ether into a methanol solution of crude [CpFe(CO)(bpy)]I. CpFe(CO)(bpy)I is very soluble in methanol and moderately soluble in water to give a red solution. Anal. for $C_{16}H_{13}FeIN_2O$ obs (calc) C 43.66 (44.48), H 2.70 (3.03), N 6.23 (6.48). ^{1}H NMR (400 MHz, CD_3CN) δ 8.87 (d, *J* = 5.2 Hz, 2H), 8.29 (d, *J* = 8.0 Hz, 2H), 8.09 (m, 2H), 7.51 (m, 2H), 4.98 ppm (s, 5H). ^{13}C NMR (100MHz, CD_3CN) δ 84.0, 118.4, 124.3, 127.0, 139.7, 158.5, 158.8 ppm. ^{1}H NMR (400 MHz, CD_3COCD_3) δ 9.18 (d, *J* = 5.6 Hz, 2H), 8.62 (d, *J* = 8.0 Hz, 2H), 8.24 (m, 2H), 7.66 (m, 2H), 5.23 ppm (s, 5H). ^{1}H NMR (400 MHz, $CDCl_3$) δ 9.05 (d, *J* = 5.2 Hz, 2H), 8.58 (d, *J* = 8.0 Hz, 2H), 8.10 (t, *J* = 7.6 Hz, 2H), 7.59 (t, *J* = 6.2 Hz, 2H), 5.04 ppm (s, 5H). IR (KBr) 1975 (CO), 1602, 1460, 1443 (Cp) cm^{-1}.

$CpFe(PTA)_2(CH_3CN)(PF_6)$. A solution of $CpFe(CO)_2Cl$ (100 mg, 0.47 mmol) in 30 mL acetonitrile was treated with PTA (163 mg, 1.04 mmol) in 20 mL of methanol. The solution was exposed to ultraviolet irradiation (Englehard-Hanovia water-cooled 450-W mercury lamp) at room temperature for 3.0 hrs under nitrogen to give a red solution. NH_4PF_6 (383 mg, 2.35 mmol) was then added to the red solution and solvent was pumped off in vacuum to dryness. The red residue was washed with cold water, dried under vacuum and then extracted with acetonitrile and layered with diethyl ether. Red crystals of $CpFe(PTA)_2(CH_3CN)(PF_6)$ which formed overnight were collected by filtration and dried under vacuum. Yield 68% (198 mg). Anal. for $C_{19}H_{32}F_6FeN_7P_3$ obs (calc) C 36.65 (36.73), H 5.19 (5.01), N 15.51(15.78). ^{1}H NMR (400 MHz, CD_3CN) δ 4.58 (m, 12H, NC*H*$_2$N), 4.36 (s, 5H, Cp), 4.10 (m, 12H, PC*H*$_2$N), 2.18 ppm (s, 3H, C*H*$_3$CN). ^{13}C NMR (100 MHz, CD_3CN) δ 56.3 (t, P*C*H$_2$N), 73.7 (s, N*C*H$_2$N), 77.0 ppm (s, Cp). ^{31}P {H} NMR (162 MHz, CD_3CN) δ -12.11 ppm (s). ^{1}H NMR (400 MHz, CD_3COCD_3) δ 4.93 (m, 12H, NC*H*$_2$N), 4.96 (s, 5H, Cp), 4.47 (m, 12H, PC*H*$_2$N), 2.43 ppm (s, 3H, C*H*$_3$CN). ^{31}P {H} NMR (162 MHz, CD_3COCD_3) δ -4.76 ppm (s). IR (KBr) 1456, 1419, 1384 (Cp), 847 (PF_6) cm^{-1}.

Crystals of **8**, **$CpFe(PTA)_3(PF_6)$** formed in the NMR tube 2 days after dissolving $CpFe(PTA)_2(CH_3CN)(PF_6)$ in D_2O.

Table S1. Comparison of Selected Bond Distance and Angles in $CpM(PTA)_2X$ Complexes.

	M = Fe X = PTA **(8)**	M = Fe X = $NCCH_3$ **(9)**	M = Ru X = Cl **ref** [2]	M =Ru X = H **ref** [3]
M-P	2.1900(5)	2.1877(7)	2.247(3)	2.2220(7)
M-P	2.1924(6)	2.2099(6)	2.258(3)	2.2267(7)
M-X	2.2013(5)	1.9099(19)	2.445(2)	1.68(7)
X-M-P	94.97(2)	89.57(6)	86.46(7)	73(2)
X-M-P	95.34(2)	91.67(6)	91.61(7)	81(2)
P-M-P	96.38(2)	96.48(2)	96.85(5)	95.68(2)
Cent-M-P	120.1(1)	123.1(1)	123.3(1)	127.3(1)
Cent-M-P	120.5(1)	124.1(1)	125.0(1)	129.0(1)
Cent-M-X	123.1(1)	122.8(1)	123.5(1)	132.5(1)

Cent = centroid of Cp ring

Comparison with other PTA complexes. As can be seen in Table S1 the M-P distances in the Fe-PTA complexes are about 0.03 to 0.05 Å shorter than in the Ru complexes. The greatest differences are in the angles the PTA ligands make around the metal. As X changes from PTA to acetonitrile to Cl to H and the metal changes from Fe to Ru the asymmetry between the two X-M-P angles within the complex increases from 0.4 to 8° and the value of the angle decreases as the bulk of the coordinated ligand decreases. The angles made by the centroid of the Cp ring, the metal and the ligands increase and become more symmetrical when the bulky PTA ligand is replaced by acetonitrile or a chloride ion independent of the metal and increase even more and become asymmetric when the hydride ligand is present.

NMR and IR Spectra

^{1}HNMR of $Fe(bpy)(P(OEt)_3)_3(CH_3CN)(OTf)_2$ in CD_3COCD_3

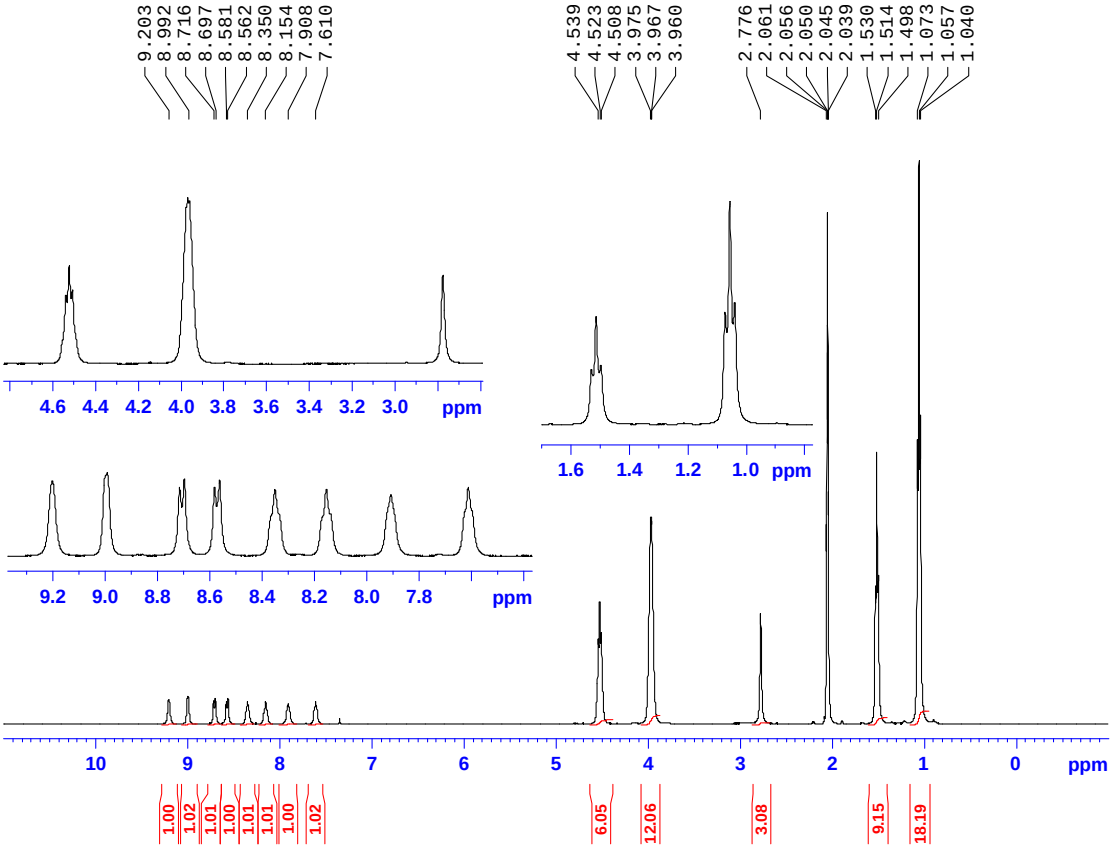

31P {H} NMR of $Fe(bpy)(P(OEt)_3)_3(CH_3CN)(OTf)_2$ in CD_3COCD_3

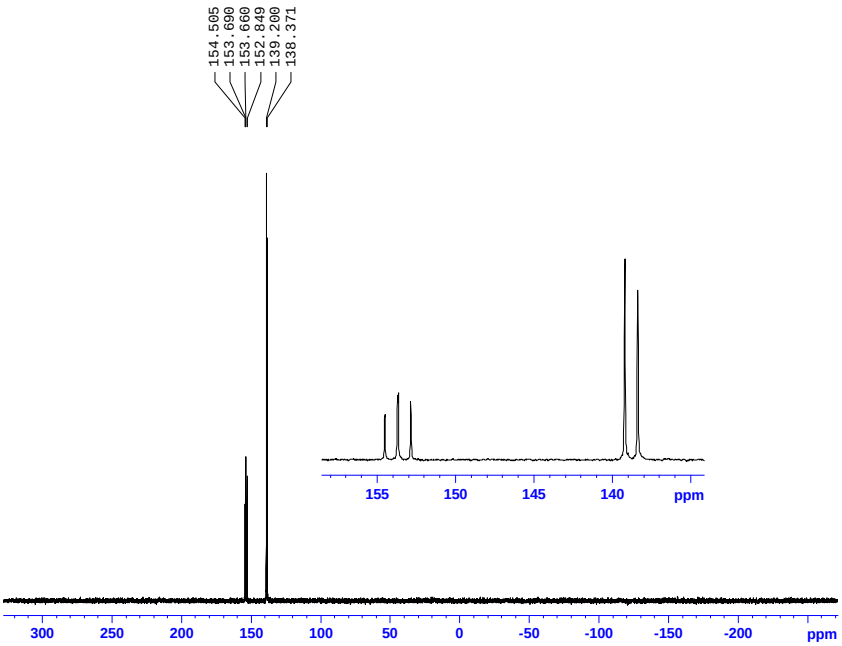

1H NMR of $Fe(bpy)(P(OEt)_3)_3(CH_3CN)(OTf)_2$ in CD_3CN

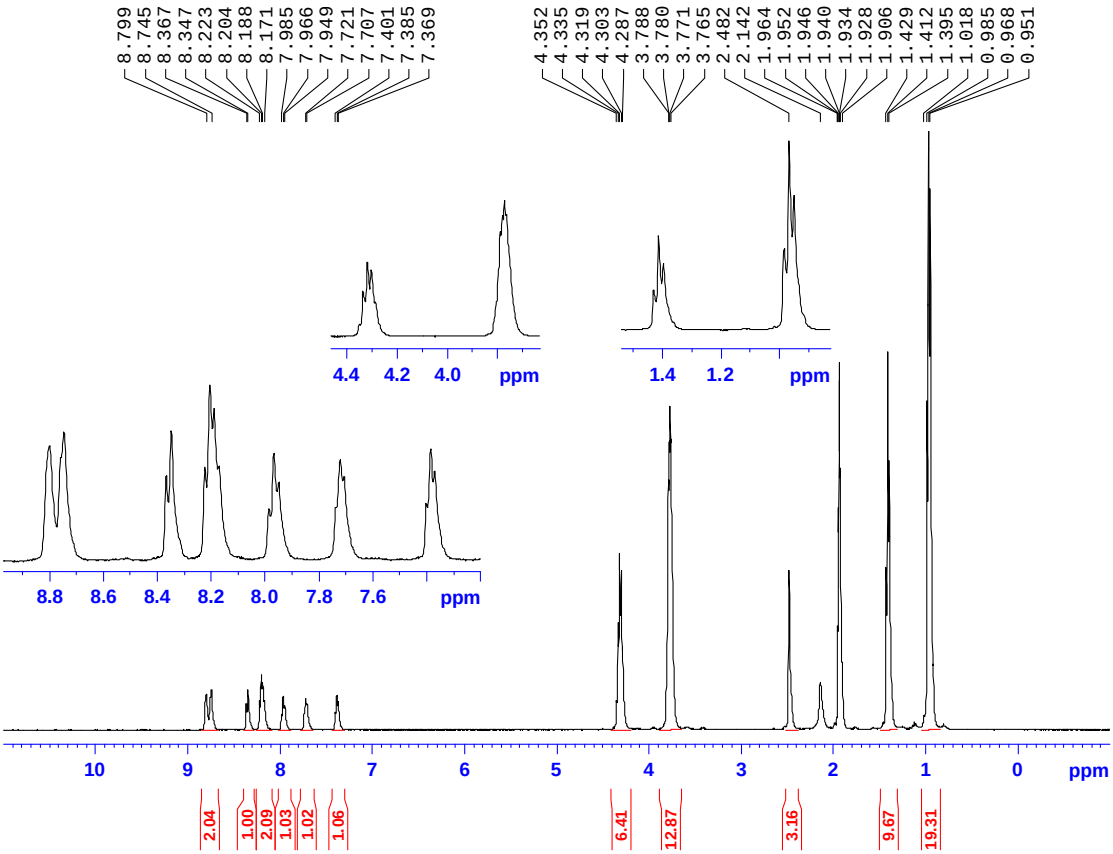

31P {H} NMR of $Fe(bpy)(P(OEt)_3)_3(CH_3CN)(OTf)_2$ in CD_3CN

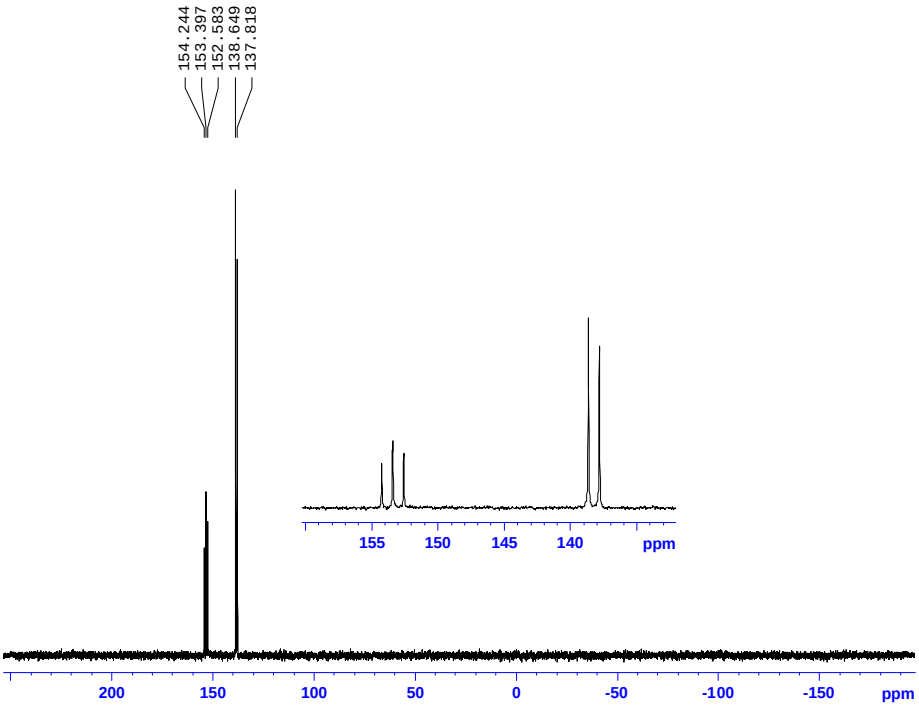

^{1}H NMR of $[Fe(Ph_2PCH_2CH=N(C_6H_4)N=CHCH_2PPh_2)(CH_3CN)_2][BPh_4]_2$ **in CD_3CN**

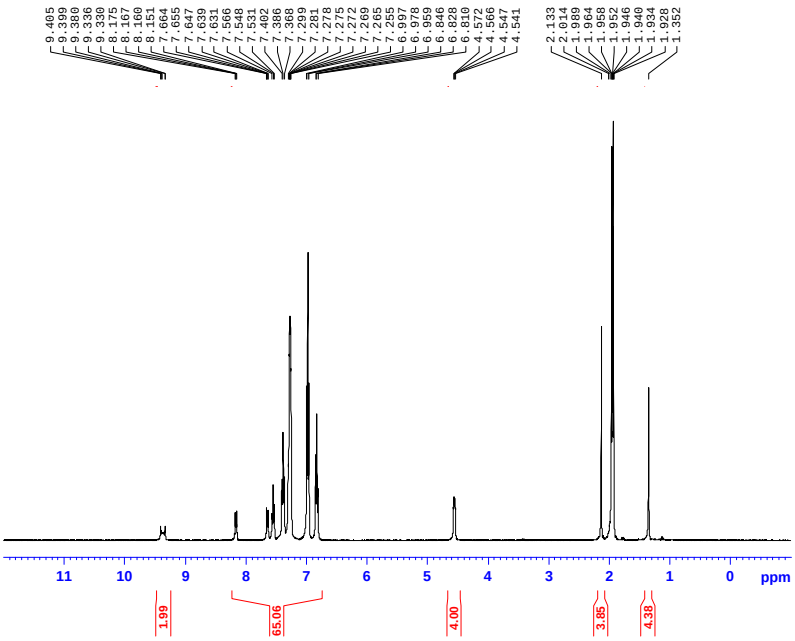

^{31}P {H} NMR of $[Fe(Ph_2PCH_2CH=N(C_6H_4)N=CHCH_2PPh_2)(CH_3CN)_2][BPh_4]_2$ in CD_3CN

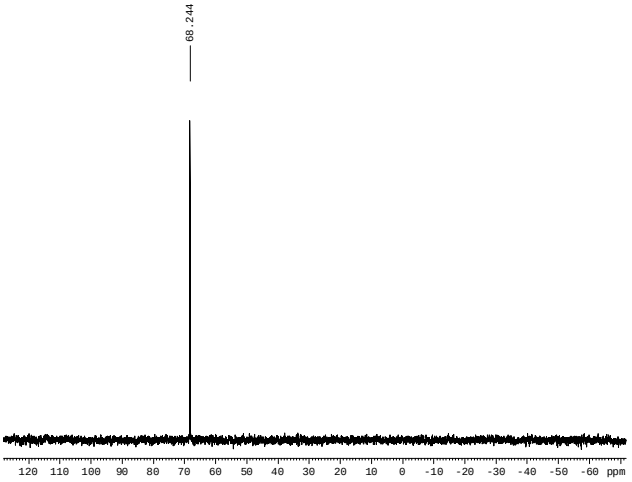

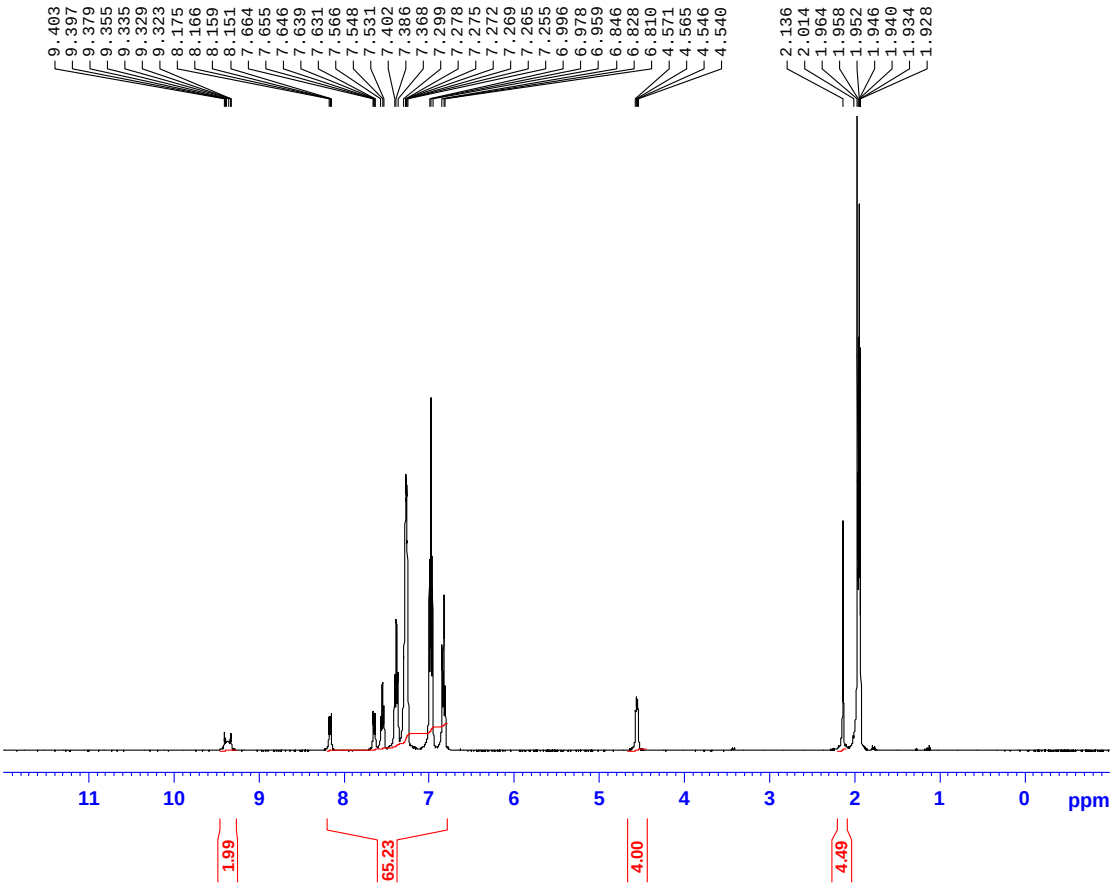

^{1}H NMR of **[Fe(Ph$_2$PCH$_2$CH=N(C$_6$H$_4$)N=CHCH$_2$PPh$_2$)(CH$_3$CN)$_2$][BPh$_4$]$_2$** in CD$_3$CN overnight, the proton peak at 1.35 ppm disappeared.

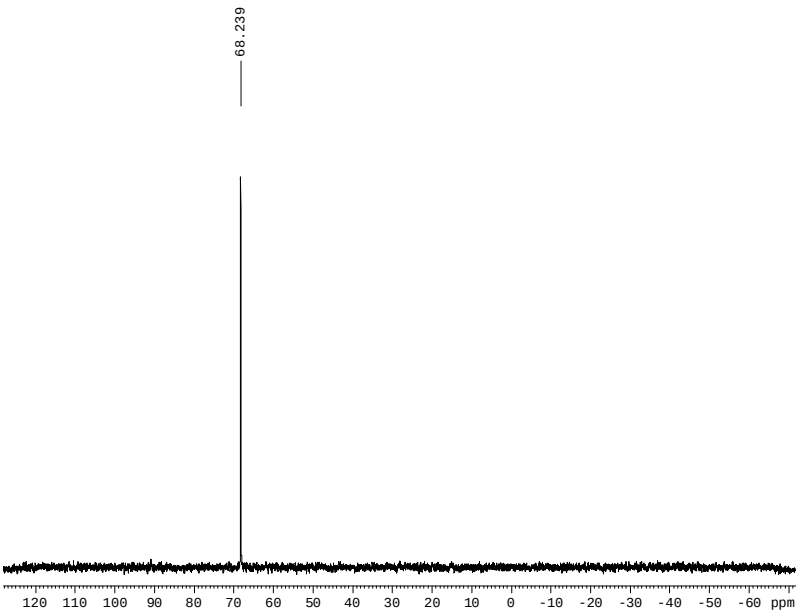

^{31}P {H} NMR of **[Fe(Ph$_2$PCH$_2$CH=N(C$_6$H$_4$)N=CHCH$_2$PPh$_2$)(CH$_3$CN)$_2$][BPh$_4$]$_2$** in CD$_3$CN overnight

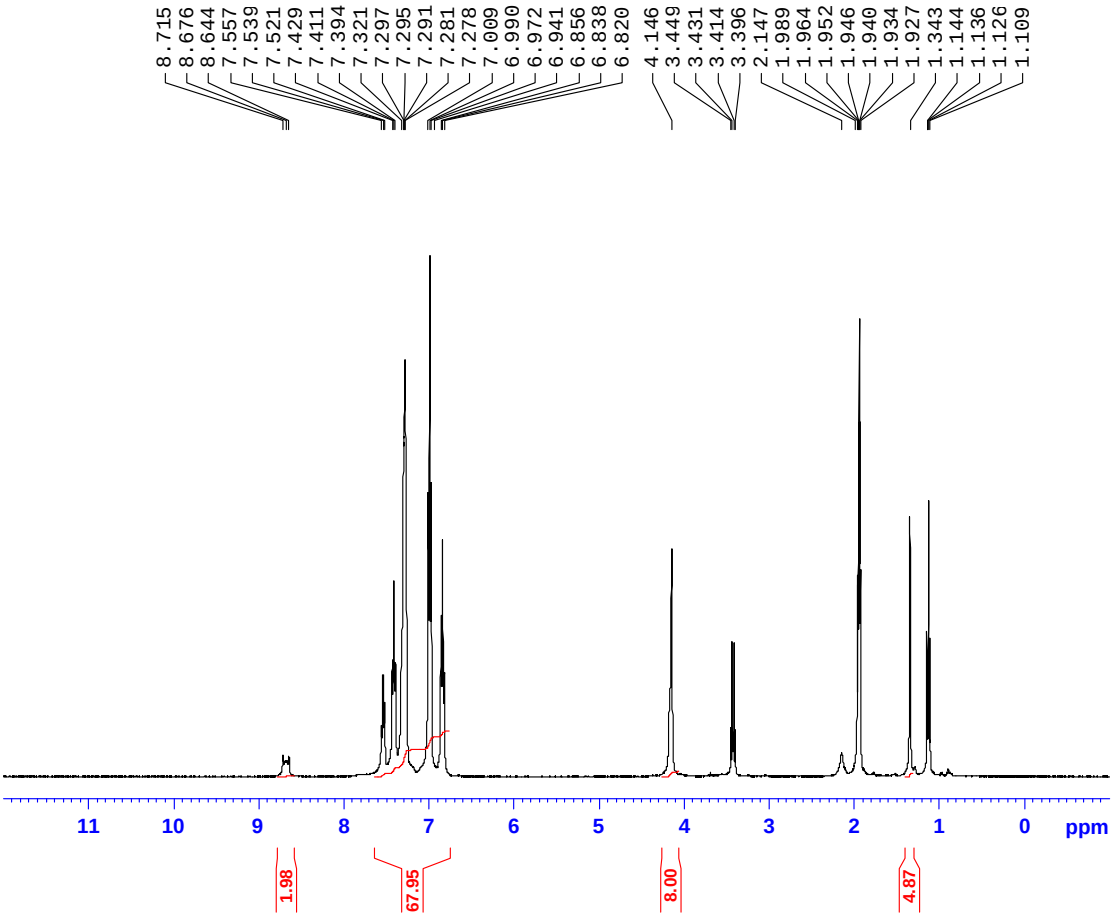

^{1}H NMR of [Fe(Ph$_2$PCH$_2$CH=NC$_2$H$_4$N=CHCH$_2$PPh$_2$)(CH$_3$CN)$_2$][BPh$_4$]$_2$ in CD$_3$CN (containing Et$_2$O)

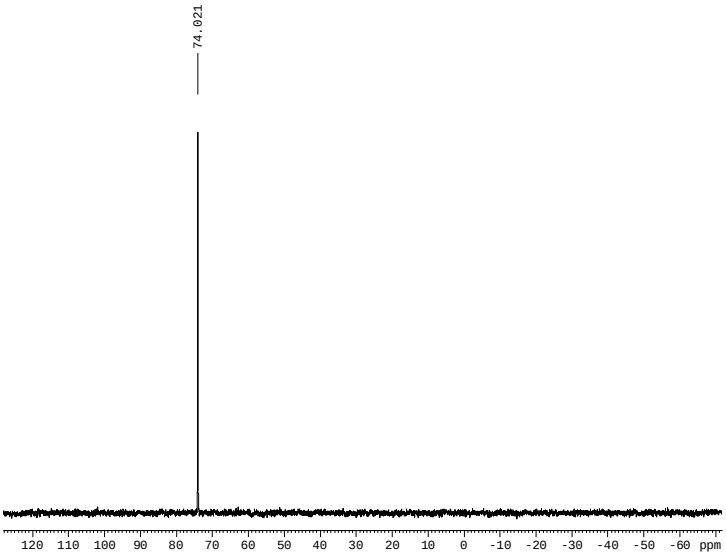

^{31}P {H} NMR of Fe(Ph$_2$PCH$_2$CH=NC$_2$H$_4$N=CHCH$_2$PPh$_2$)(CH$_3$CN)$_2$][BPh$_4$]$_2$ in CD$_3$CN

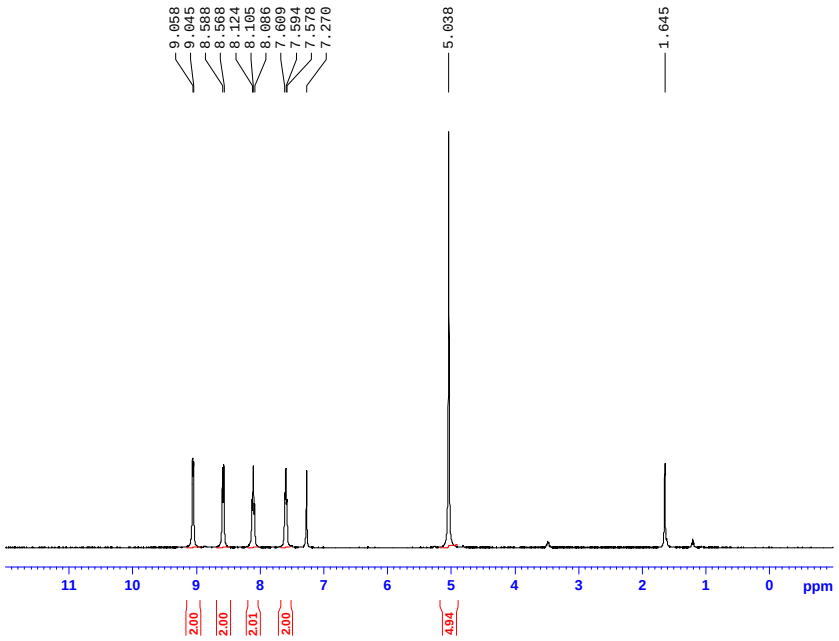

^{1}H NMR of [CpFe(bpy)(CO)]I in $CDCl_3$

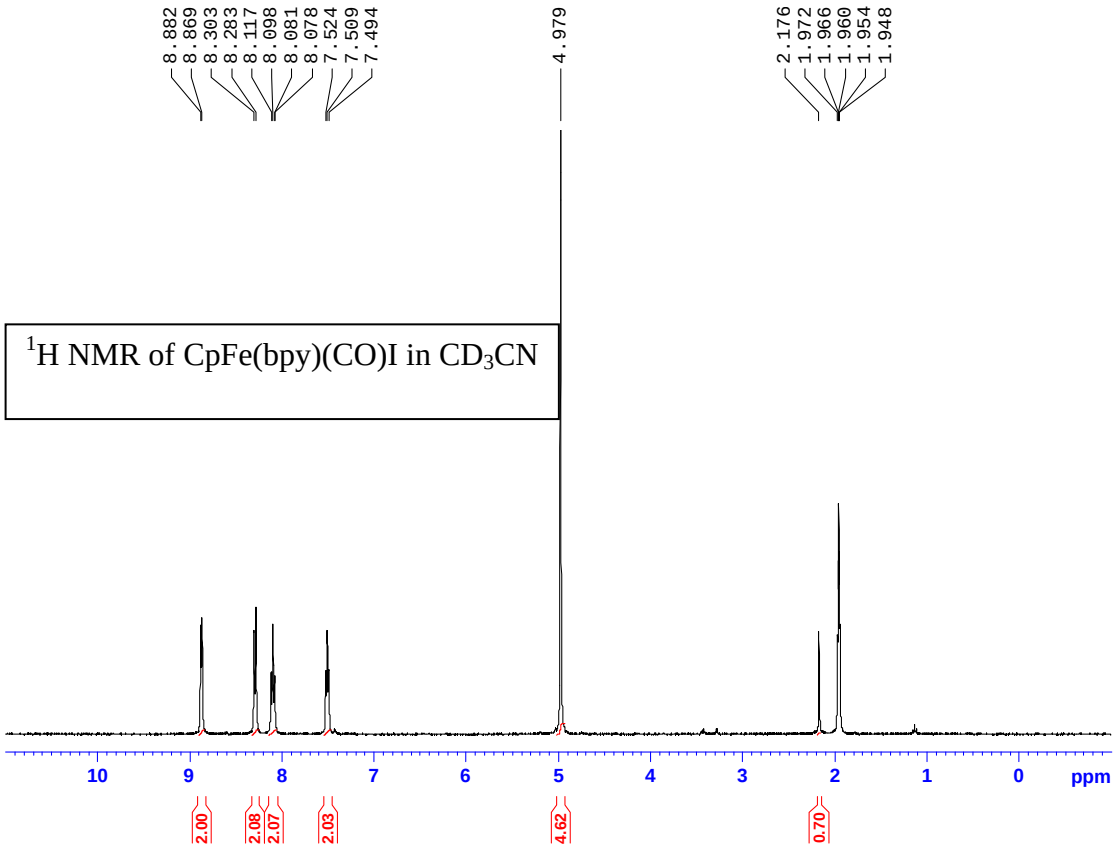

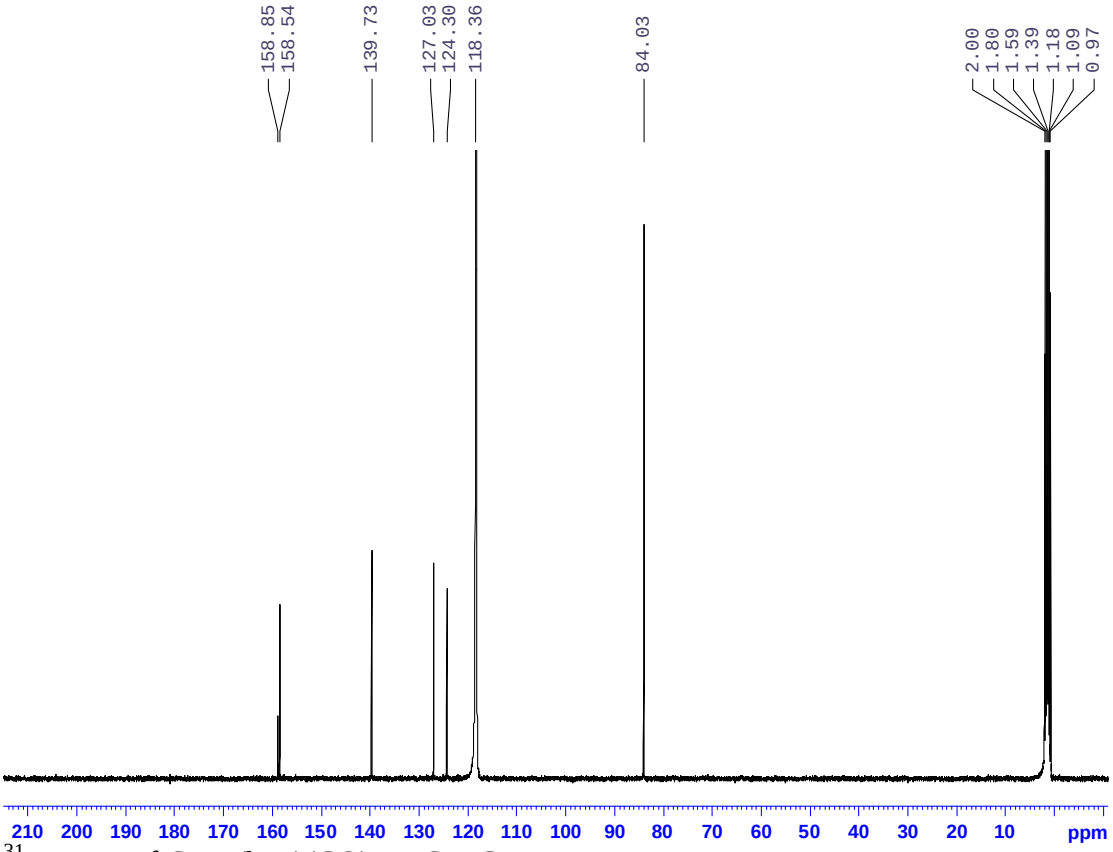

^{31}P NMR of CpFe(bpy)(CO)I in CD_3CN

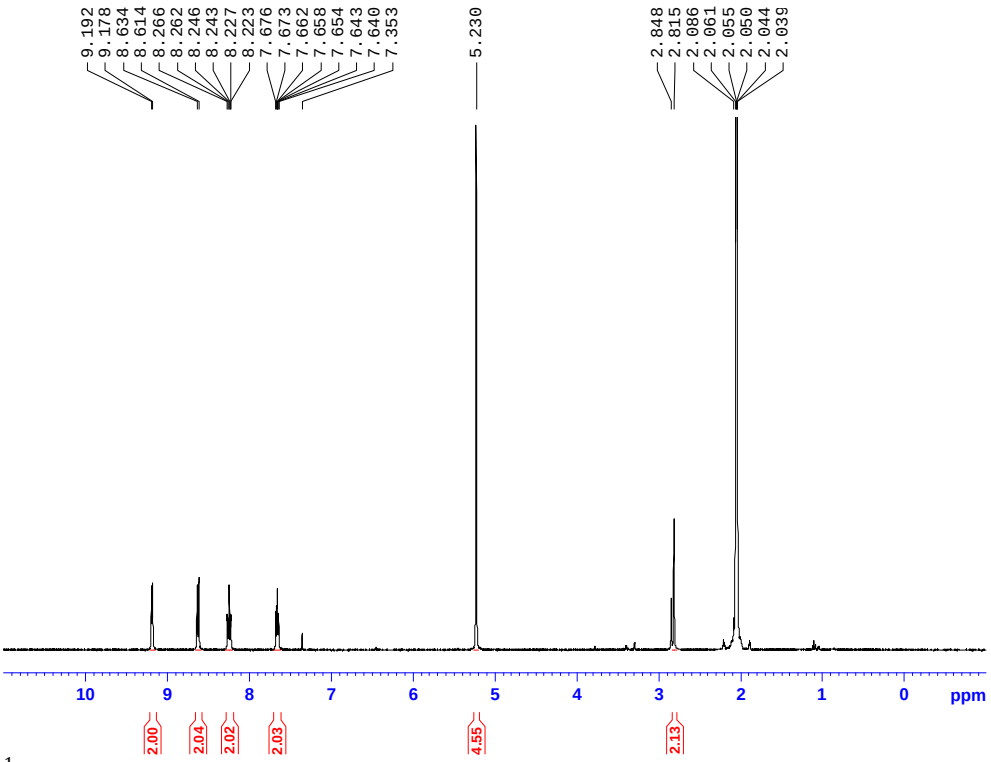

^{1}H NMR of [CpFe(bpy)(CO)]I in CD_3COCD_3

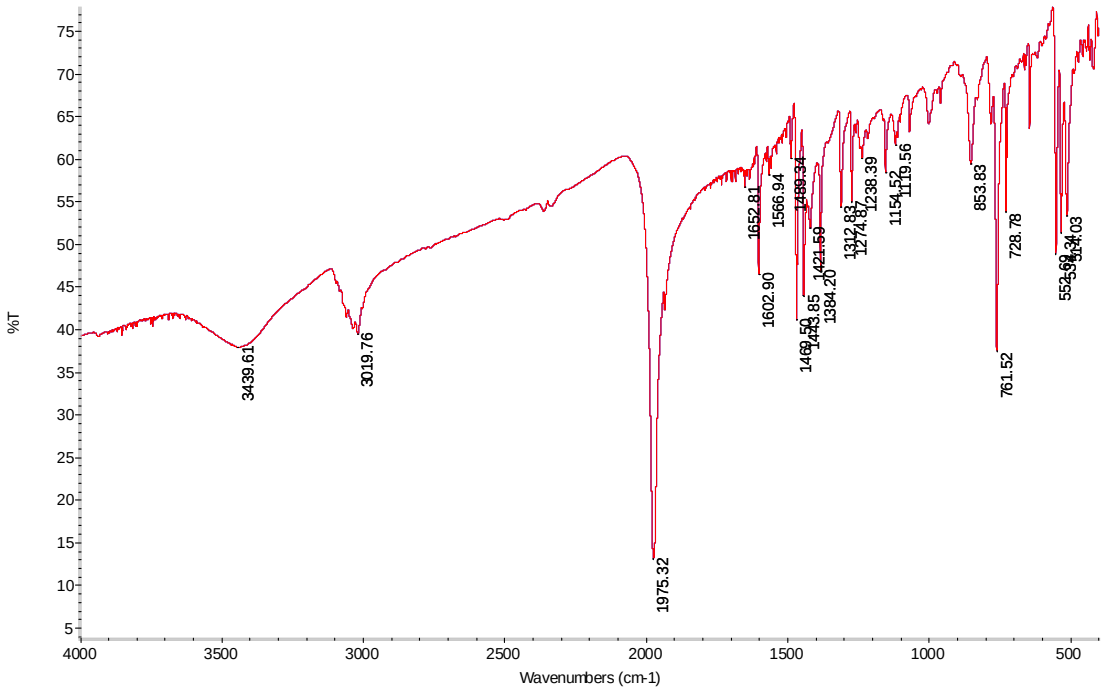

IR (KBr cm^{-1}) of [CpFe(CO)(bpy)]I

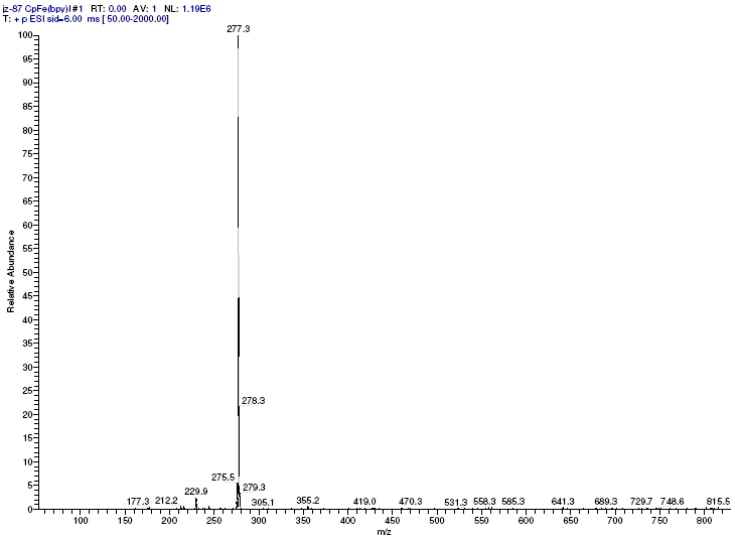

MS of CpFe(CO)(bpy)I

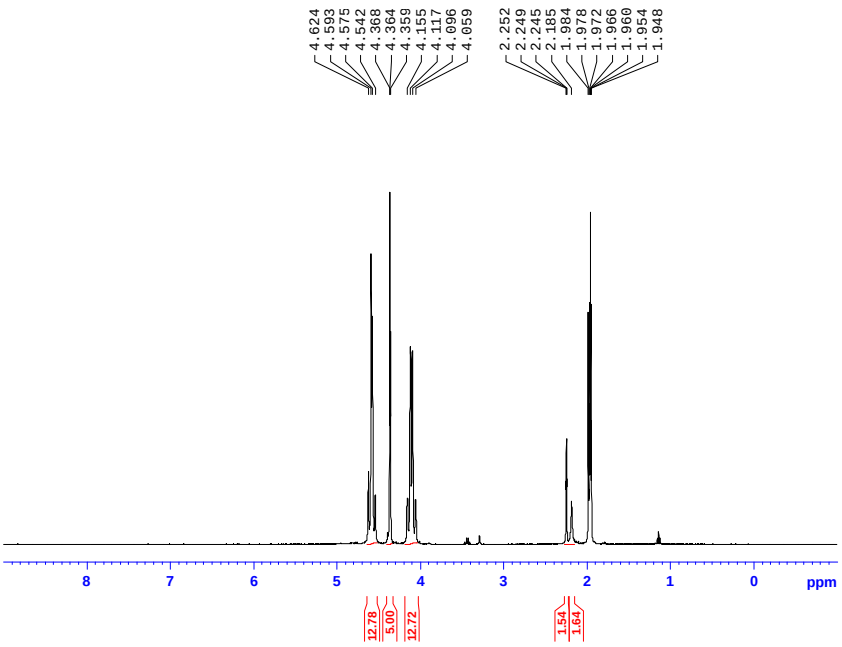

^{1}H NMR of CpFe(PTA)$_2$(CH$_3$CN)(PF$_6$) in CD$_3$CN

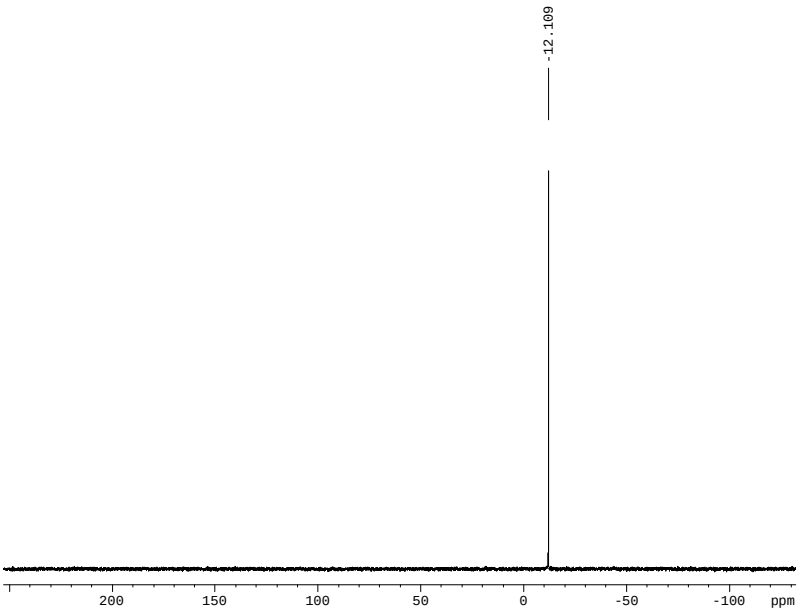

^{31}P {H} NMR of CpFe(PTA)$_2$(CH$_3$CN)(PF$_6$) in CD$_3$CN

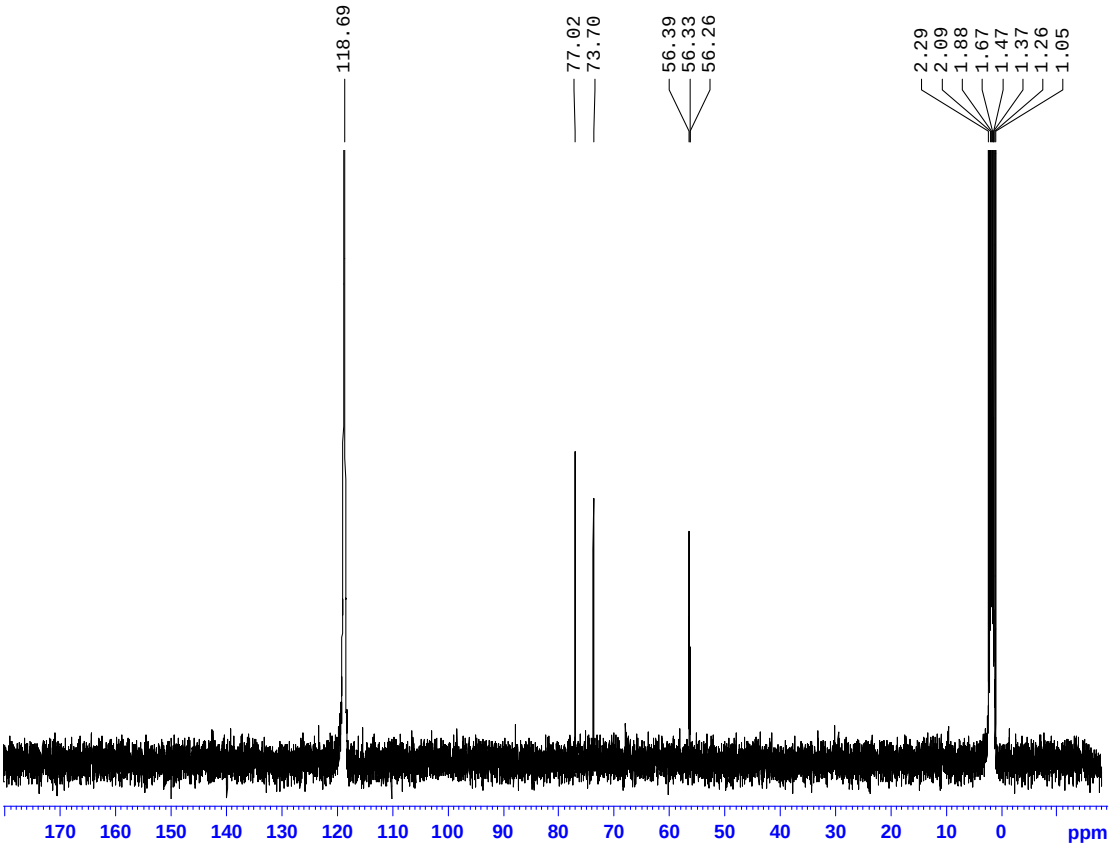

^{13}C {H} NMR of CpFe(PTA)$_2$(CH$_3$CN)(PF$_6$) in CD$_3$CN

IR (KBr cm^{-1}) of CpFe(PTA)$_2$(CH$_3$CN)(PF$_6$)

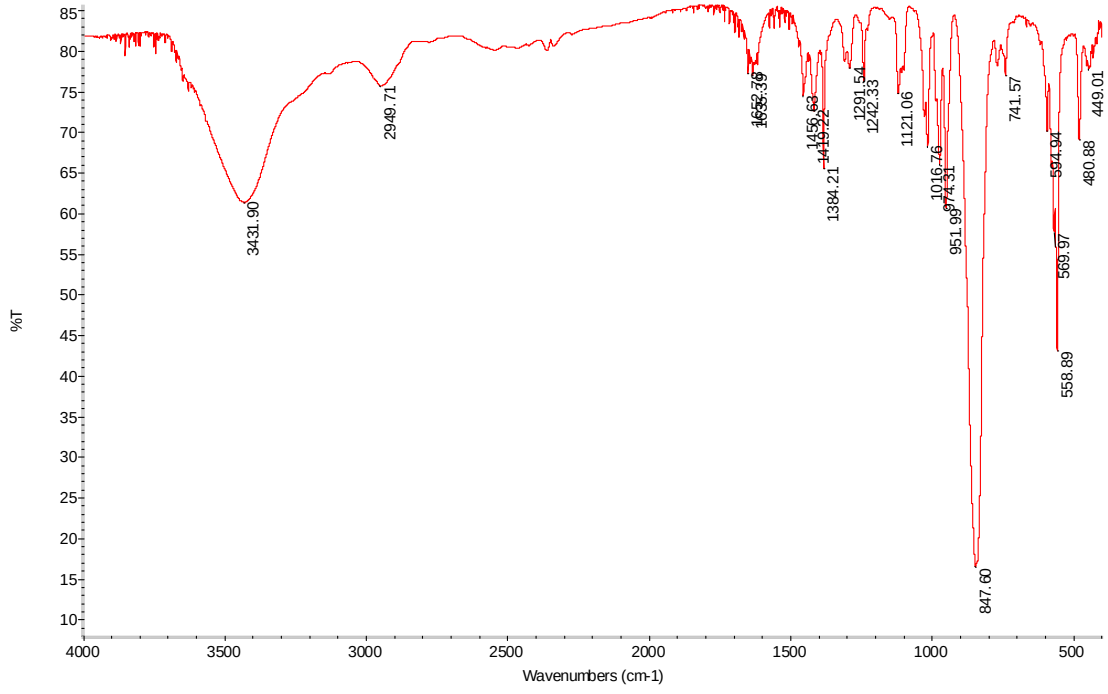

^{1}H NMR of $CpFe(PTA)_2(CH_3CN)(PF_6)$ in CD_3COCD_3

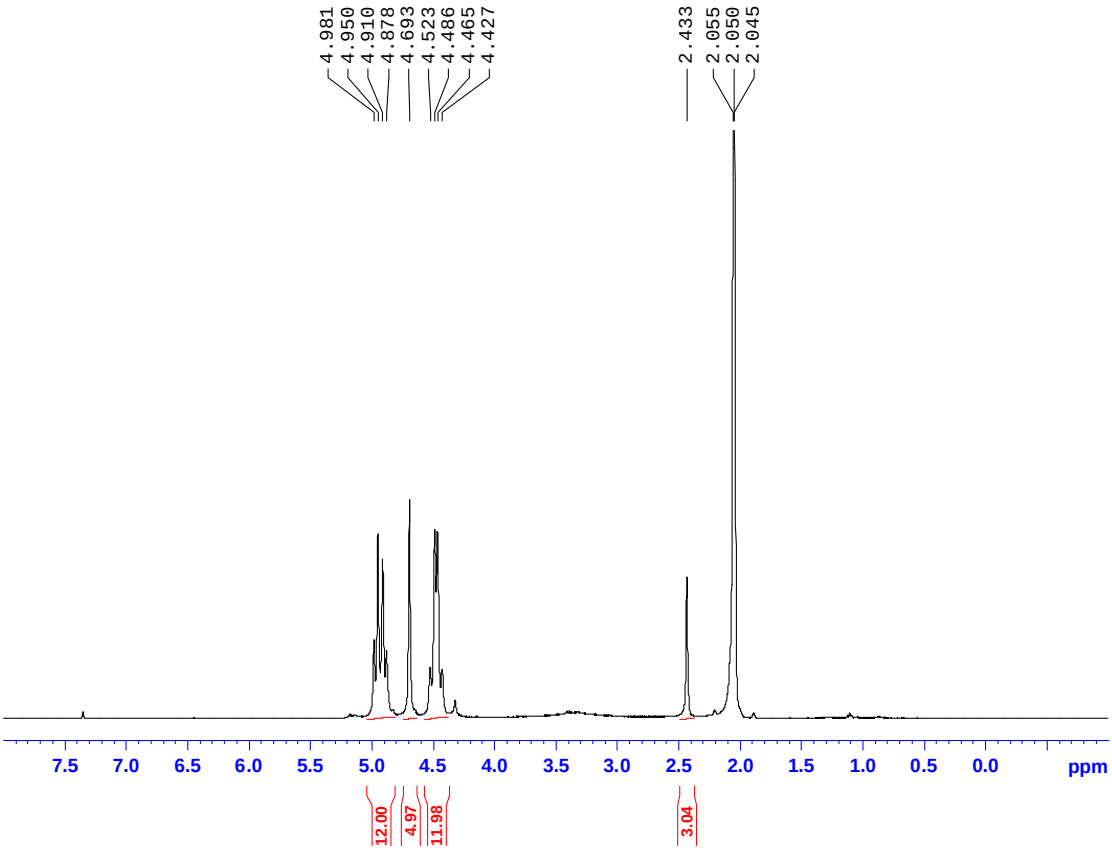

^{31}P {H} NMR of $CpFe(PTA)_2(CH_3CN)(PF_6)$ in CD_3COCD_3

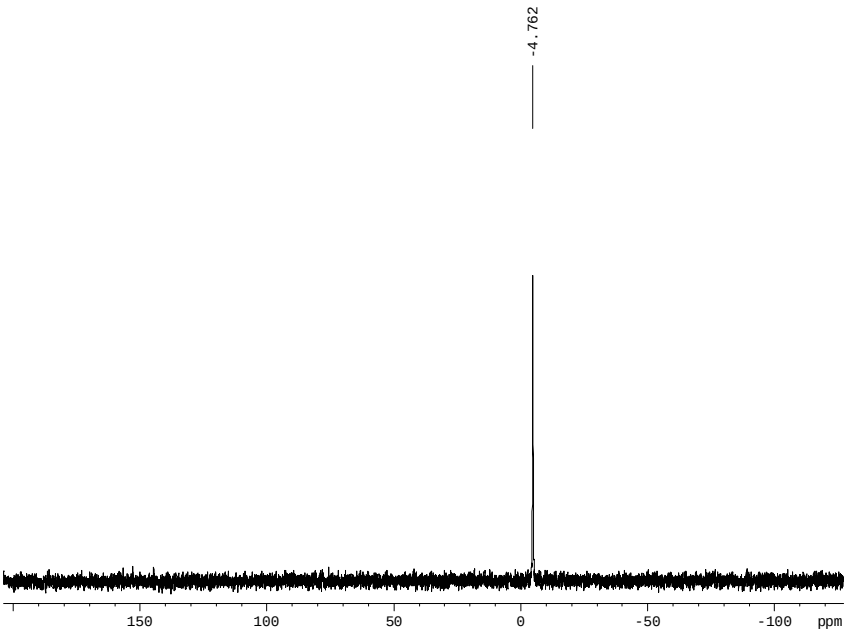

Spectral changes for $CpFe(PTA)_2(CH_3CN)(PF_6)$ in D_2O over 2 days

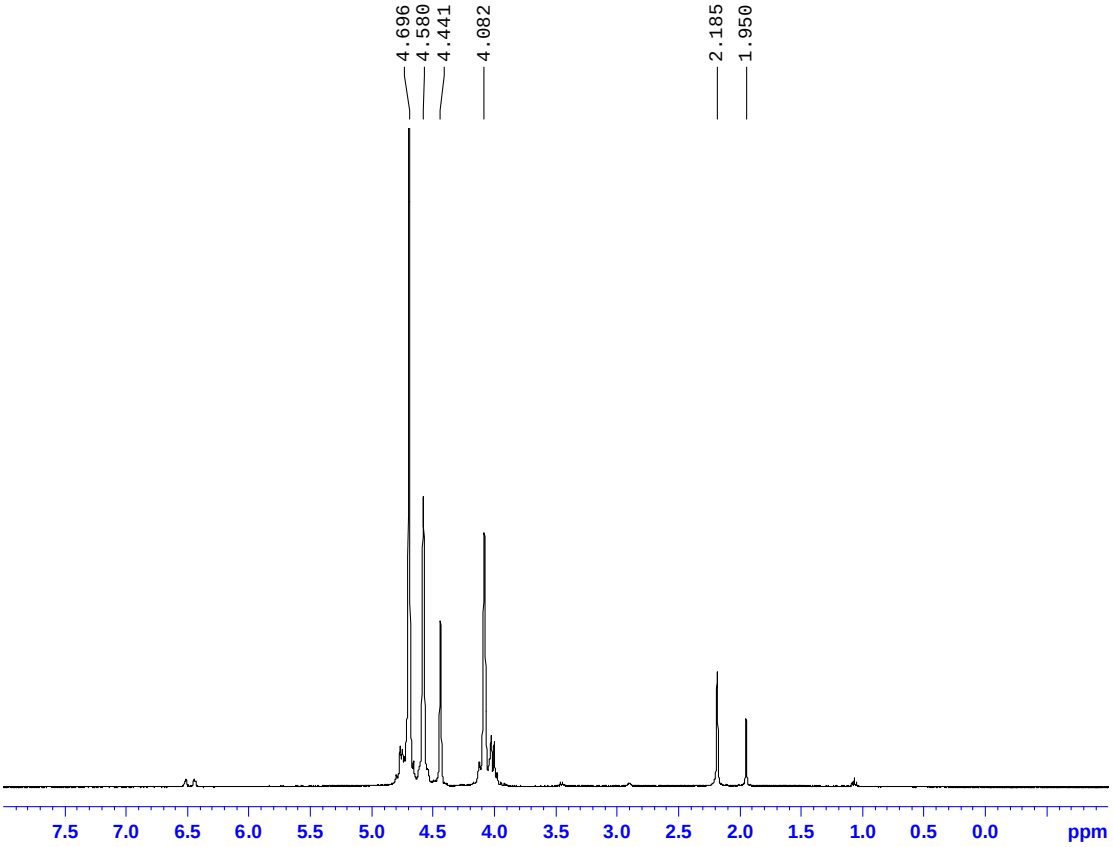

^{1}H NMR of $CpFe(PTA)_2(CH_3CN)(PF_6)$ in D_2O initially

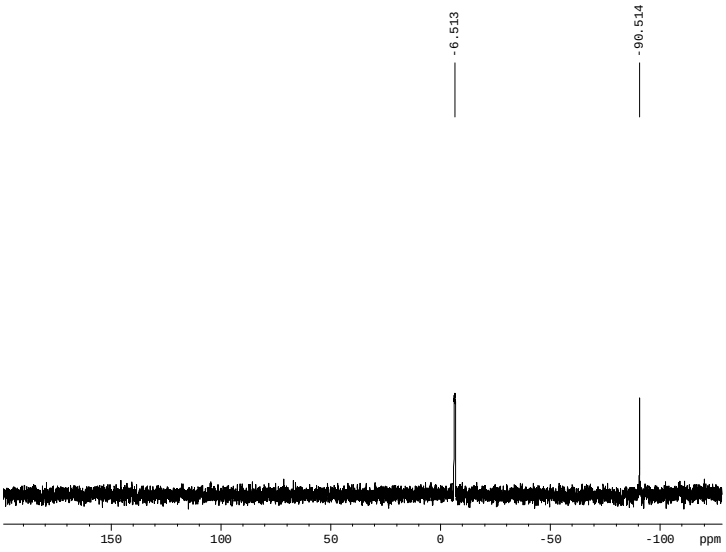

^{31}P {H} NMR of $CpFe(PTA)_2(CH_3CN)(PF_6)$ in D_2O

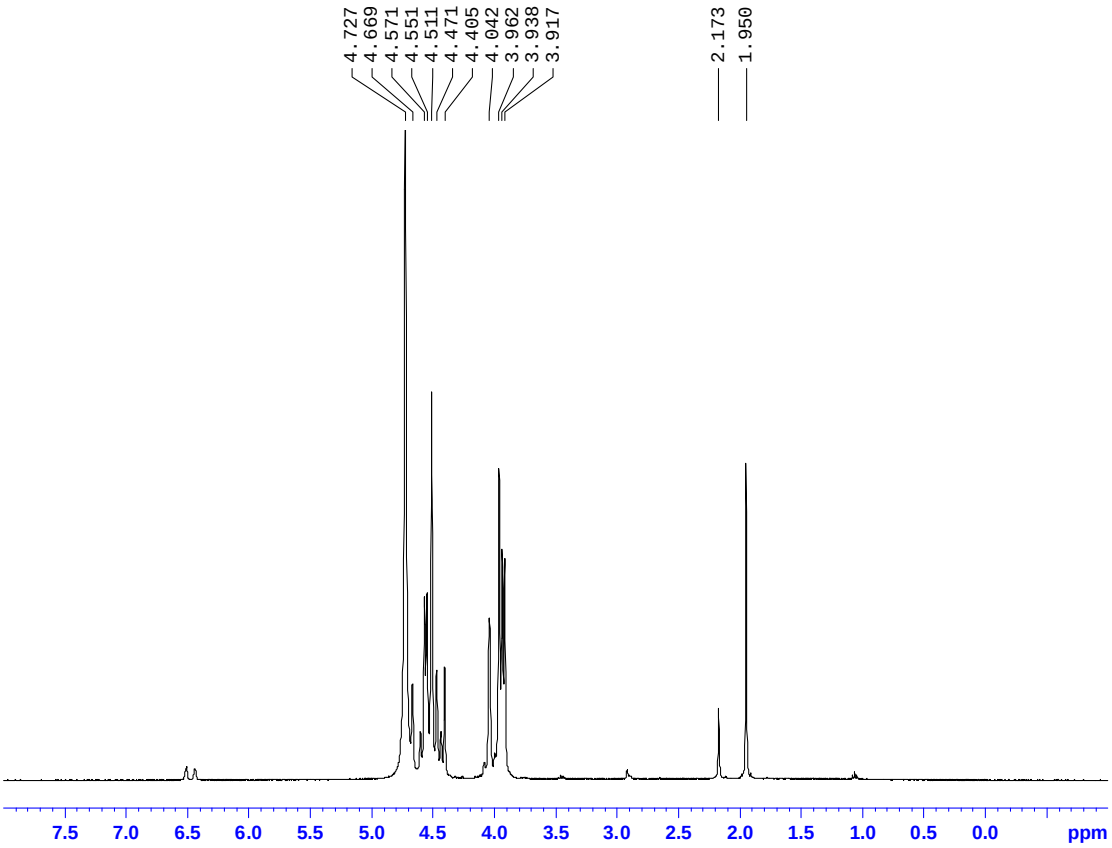

^{1}H NMR of CpFe(PTA)$_2$(CH$_3$CN)(PF$_6$) in D$_2$O for 1 day

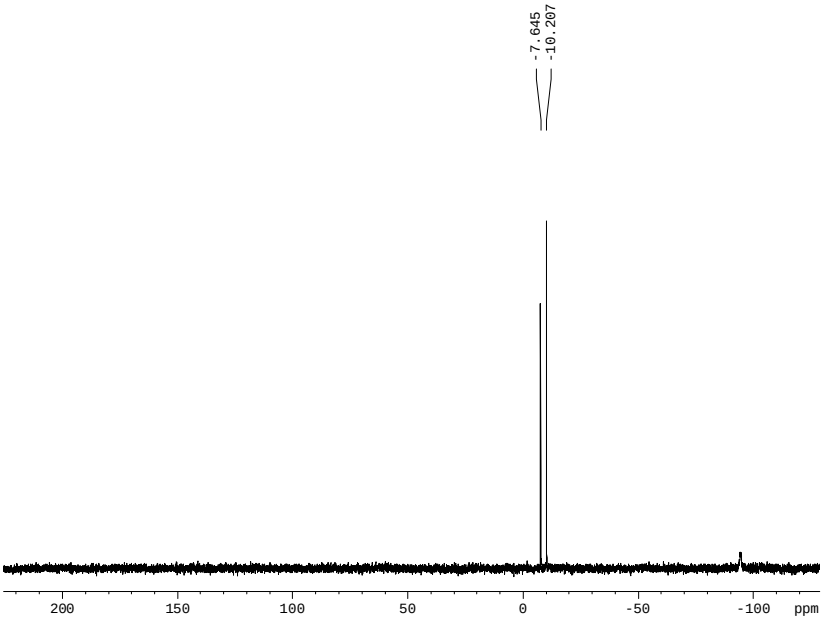

^{31}P {H} NMR of CpFe(PTA)$_2$(CH$_3$CN)(PF$_6$) in D$_2$O for 1 day

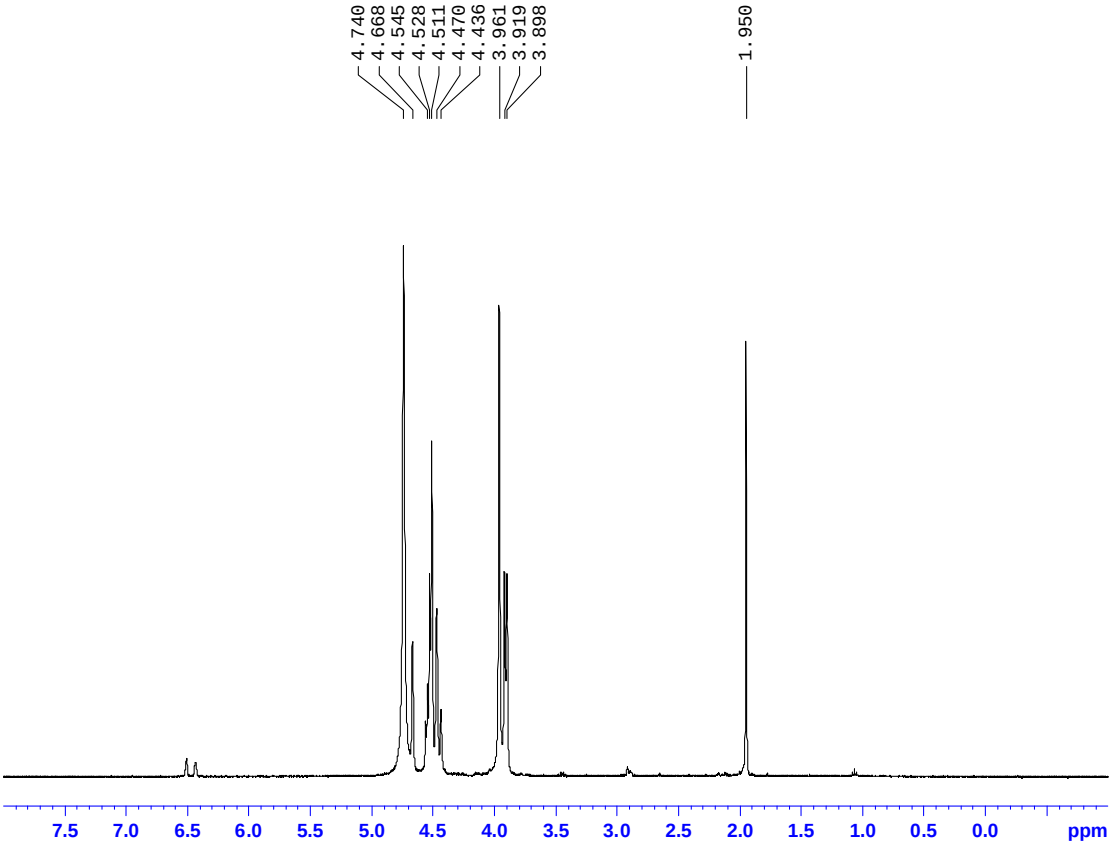

^{1}H NMR of CpFe(PTA)$_2$(CH$_3$CN)(PF$_6$) in D$_2$O for 2 days

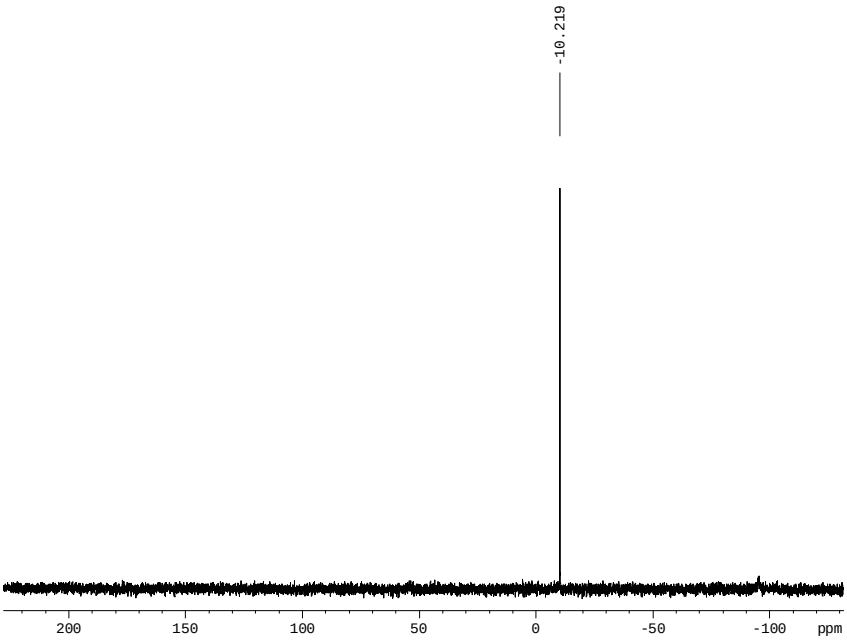

^{31}P {H} NMR of CpFe(PTA)$_2$(CH$_3$CN)(PF$_6$) in D$_2$O for 2 days

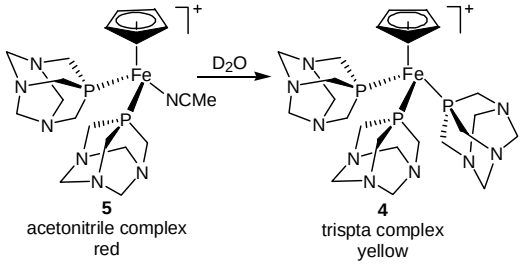

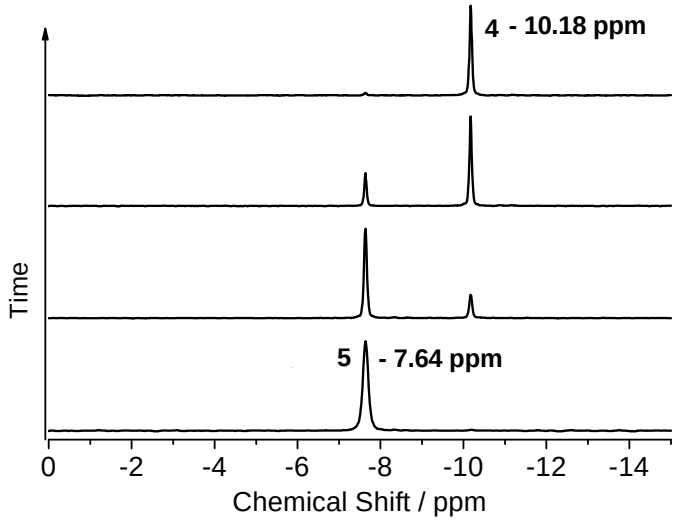

^{31}P NMR of $CpFe(PTA)_2(CH_3CN)(PF_6)$ in D_2O

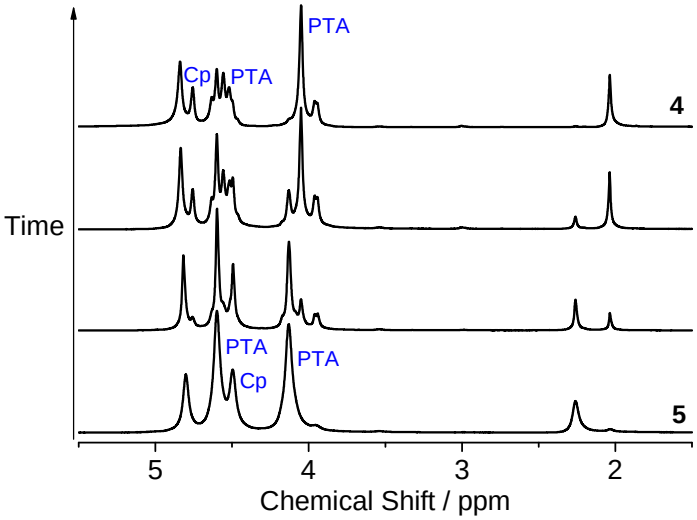

^{1}H NMR of $CpFe(PTA)_2(CH_3CN)(PF_6)$ in D_2O

ESI Mass Spectra

$Fe(bpy)(P(OEt)_3)_3(H)(OTf)$

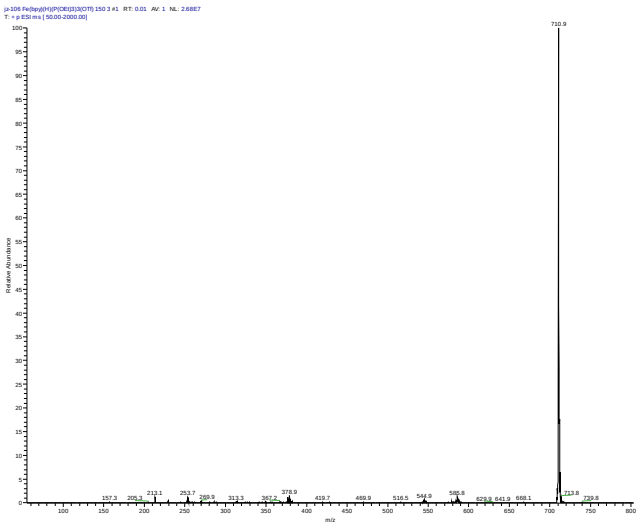

Fe(bpy)(H)(P(OEt)3)3(OTf) Conditions: Sheath Gas Flow Rate 5, Auxiliary Gas Flow Rate 0, Spray Voltage 3.0 KV, Capillary Temperature 150, Capillary Voltage 24, Tube Lens Offset Voltage 35
$Fe(bpy)(H)(P(OEt)3)3^+$ m/e = 710.9

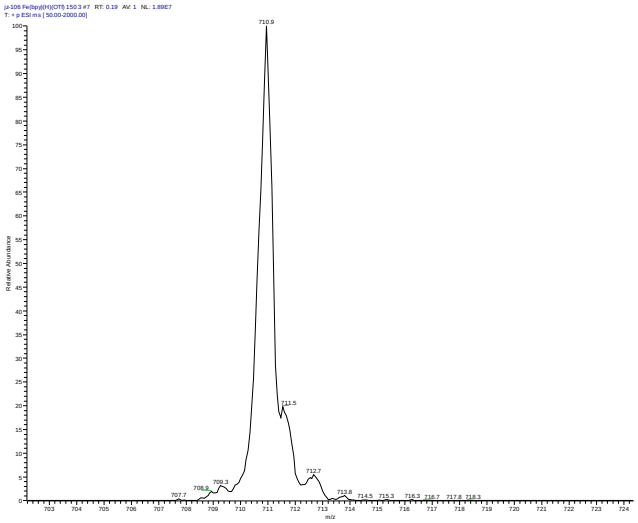

Fe(bpy)(H)(P(OEt)3)3(OTf) Conditions: Sheath Gas Flow Rate 5, Auxiliary Gas Flow Rate 0, Spray Voltage 3.0 KV, Capillary Temperature 150, Capillary Voltage 24, Tube Lens Offset Voltage 35

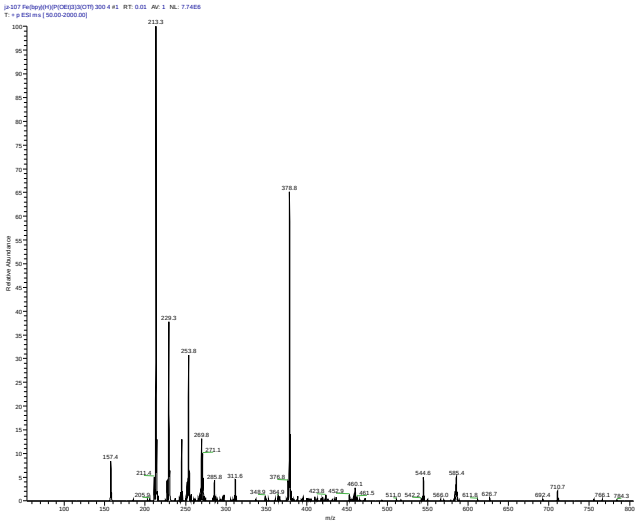

Fe(bpy)(H)(P(OEt)3)3(OTf) Conditions: Sheath Gas Flow Rate 20, Auxiliary Gas Flow Rate 20, Spray Voltage 4.0 KV, Capillary Temperature 300, Capillary Voltage 24, Tube Lens Offset Voltage 35
M^+ $[Fe(bpy)(H)(P(OEt)3)3]^+$ m/e = 710.9
M^+ - P(OEt)3 m/e = 544.6
M^+ - 2 P(OEt)3 m/e = 378.8
M^+ - 3 P(OEt)3 m/e = 213.3

Ru(bpy)(H)(P(OEt)3)3(PF_6)

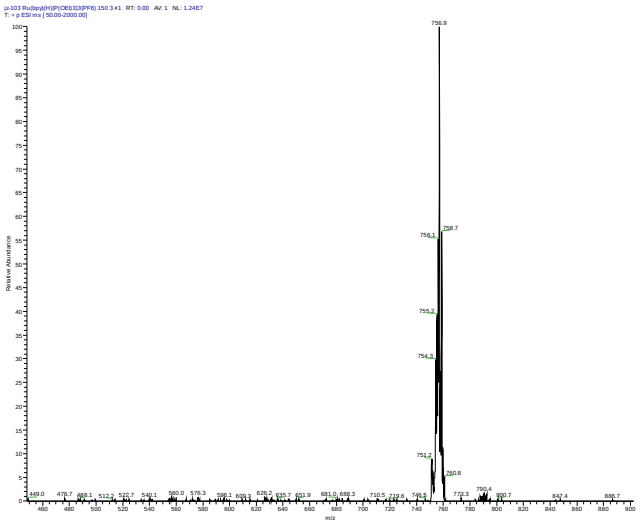

Ru(bpy)(H)(P(OEt)3)3(PF_6) Conditions: Sheath Gas Flow Rate 5, Auxiliary Gas Flow Rate 0, Spray Voltage 3.0 KV, Capillary Temperature 150, Capillary Voltage 24, Tube Lens Offset Voltage 35
M^+ $[Ru(bpy)(H)(P(OEt)3)3]^+$ m/e = 756.9

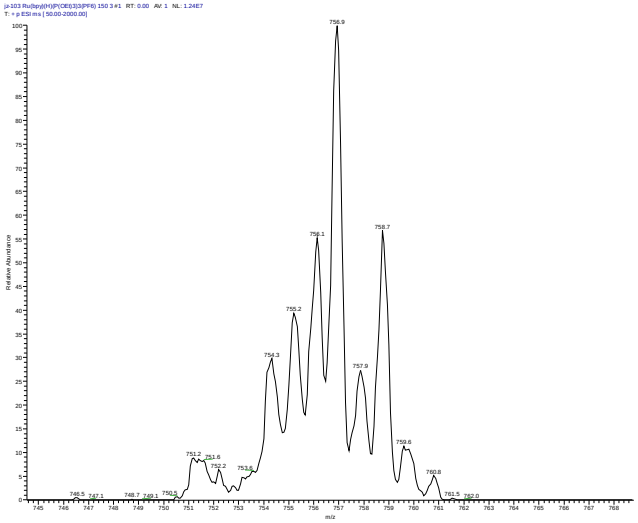

Ru(bpy)(H)(P(OEt)3)3(PF_6) Conditions: Sheath Gas Flow Rate 5, Auxiliary Gas Flow Rate 0, Spray Voltage 3.0 KV, Capillary Temperature 150, Capillary Voltage 24, Tube Lens Offset Voltage 35

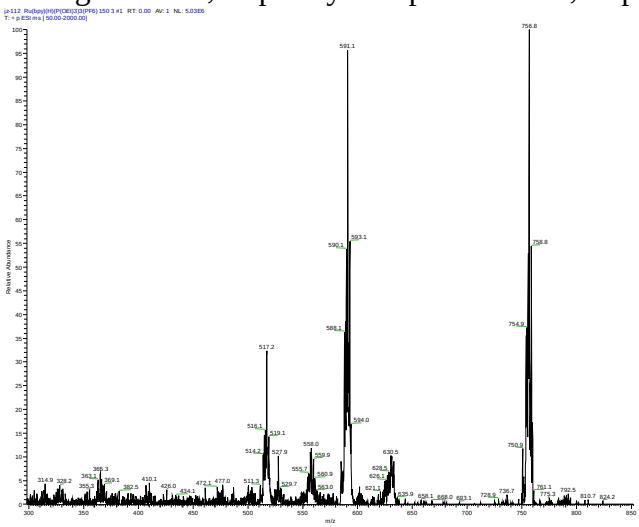

Ru(bpy)(H)(P(OEt)3)3(PF_6) Conditions: Sheath Gas Flow Rate 5, Auxiliary Gas Flow Rate 0, Spray Voltage 4.0 KV, Capillary Temperature 150, Capillary Voltage 24, Tube Lens Offset Voltage 35

M^+ $[Ru(bpy)(H)(P(OEt)_3)_3]^+$ m/e = 756.9

M^+ - $P(OEt)_3$ m/e = 591.1

$Ru(bpy)_2(H)(P(OEt)_3)(PF_6)$

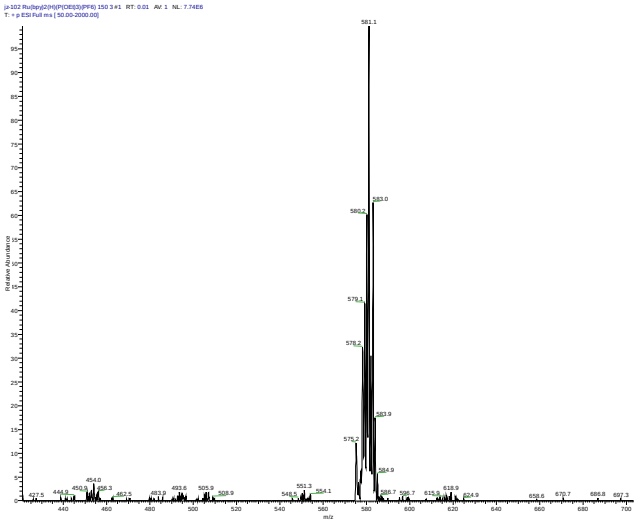

$Ru(bpy)2(H)(P(OEt)_3)(PF_6)$ Conditions: Sheath Gas Flow Rate 5, Auxiliary Gas Flow Rate 0, Spray Voltage 3.0 KV, Capillary Temperature 150, Capillary Voltage 24, Tube Lens Offset Voltage 35
M^+ $[Ru(bpy)2(H)(P(OEt)_3)]^+$ m/e = 581.1

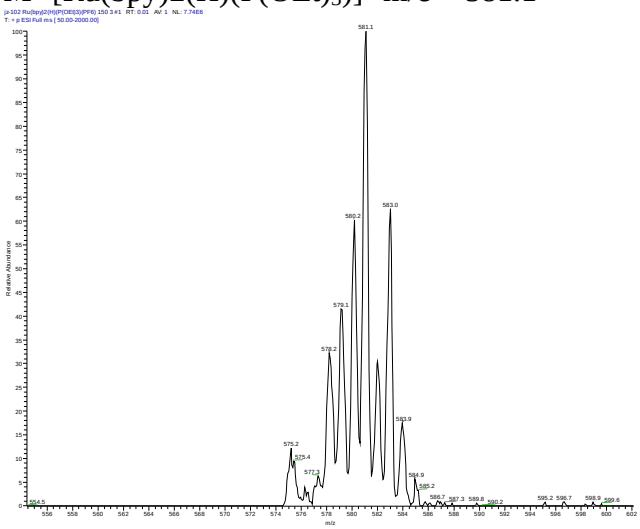

$Ru(bpy)2(H)(P(OEt)_3)(PF_6)$ Conditions: Sheath Gas Flow Rate 5, Auxiliary Gas Flow Rate 0, Spray Voltage 3.0 KV, Capillary Temperature 150, Capillary Voltage 24, Tube Lens Offset Voltage 35

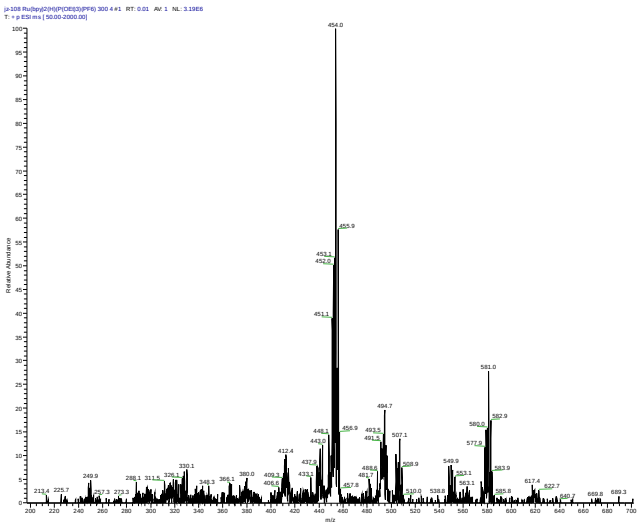

Ru(bpy)2(H)(P(OEt)$_3$)(PF$_6$) Conditions: Sheath Gas Flow Rate 20, Auxiliary Gas Flow Rate 20, Spray Voltage 4.0 KV, Capillary Temperature 300, Capillary Voltage 24, Tube Lens Offset Voltage 35
M$^+$ [Ru(bpy)2(H)(P(OEt)$_3$)(PF$_6$)]$^+$ m/e = 581.1

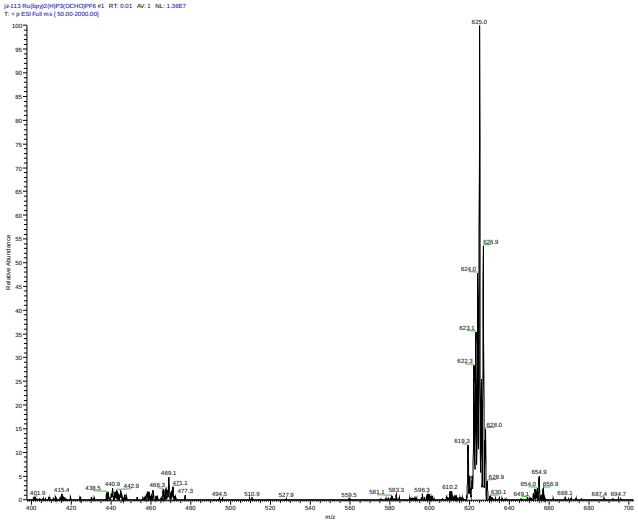

Ru(bpy)2(H)(P(OEt)$_3$)(PF$_6$) + CO2 in methanol, 150 3.RAW, Conditions: Sheath Gas Flow Rate 5, Auxiliary Gas Flow Rate 0, Spray Voltage 3.0 KV, Capillary Temperature 150, Capillary Voltage 24, Tube Lens Offset Voltage 35
M$^+$ [Ru(bpy)2(OCHO)(P(OEt)$_3$)]$^+$ m/e = 625.0

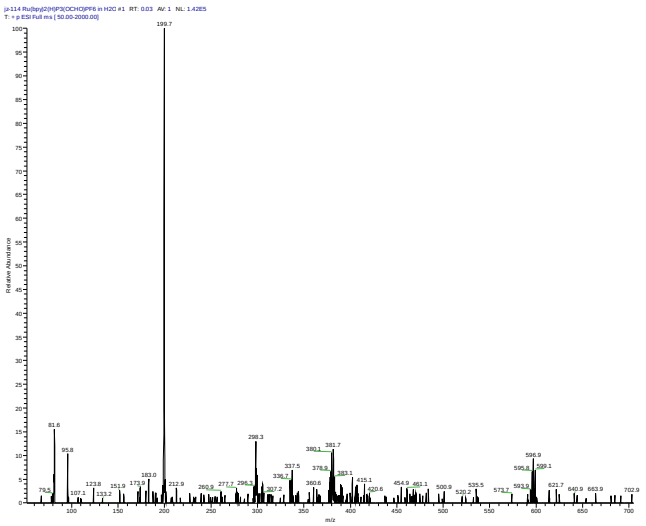

$Ru(bpy)_2(H)(P(OEt)_3)(PF_6)$ + CO_2 in water, 150 3.RAW
Conditions: Sheath Gas Flow Rate 5, Auxiliary Gas Flow Rate 0, Spray Voltage 3.0 KV, Capillary Temperature 150, Capillary Voltage 24, Tube Lens Offset Voltage 35
M+ [$Ru(bpy)2(OH)(P(OEt)_3)$] m/e = 596.9
M+/2 m/e = 298.3
M+/3 m/e = 199.7

Reactions of reduced M(bpy)(P(OEt)$_3$)(H) complexes with CO_2 in acetonitrile.

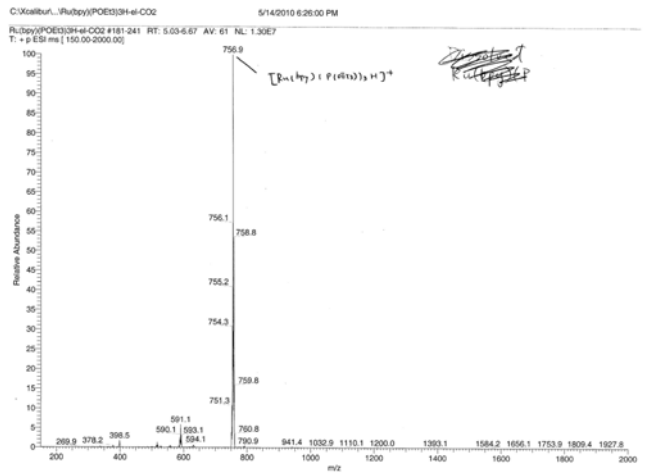

Solution from Na-Hg reduced $Ru(bpy)(P(OEt)_3)_3(H)^+$ + CO_2.

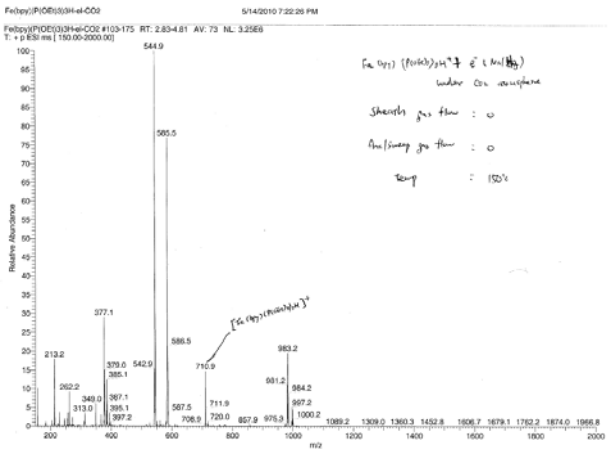

Solution from Na-Hg reduced $Fe(bpy)(P(OEt)_3)_3(H)^+ + CO_2$.

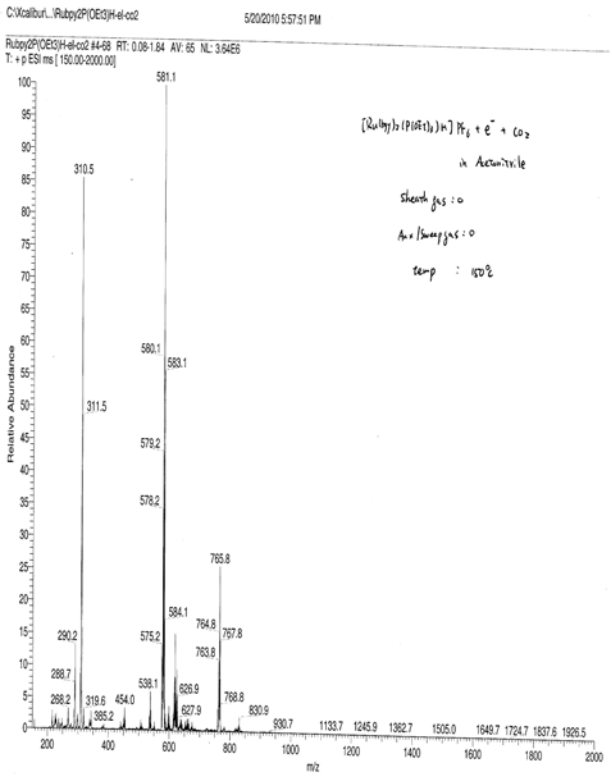

Solution from Na-Hg reduced $Ru(bpy)_2(P(OEt)_3)(H)^+ + CO_2$.

UV-Vis Spectra

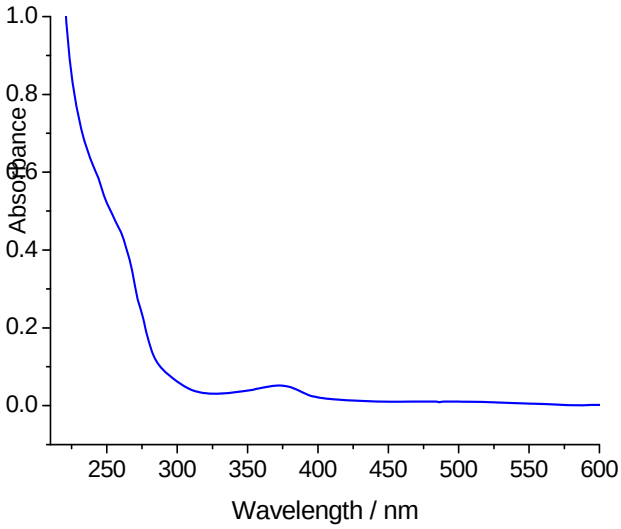

$[Fe(Ph_2PCH_2CH=N(C_6H_4)N=CHCH_2PPh_2)(CH_3CN)_2](BPh_4)_2$, 9.34 $\times 10^{-6}$ M in CH_3CN.

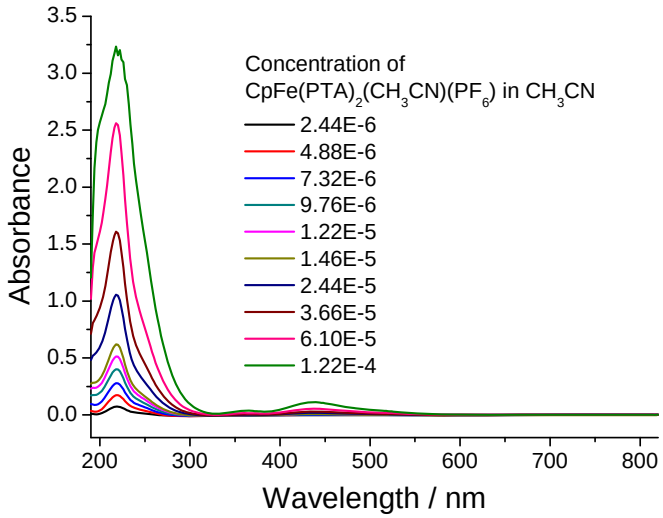

$CpFe(PTA)_2(CH_3CN)(PF_6)$ in CH_3CN

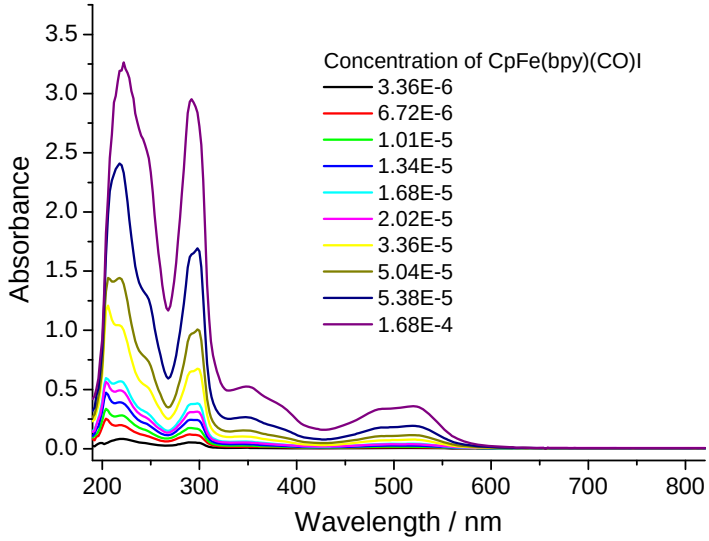

[CpFe(bpy)(CO)]I in MeOH

Fe(bpy)(P(OEt)$_3$)$_3$(H)(OTf) in CH$_3$CN

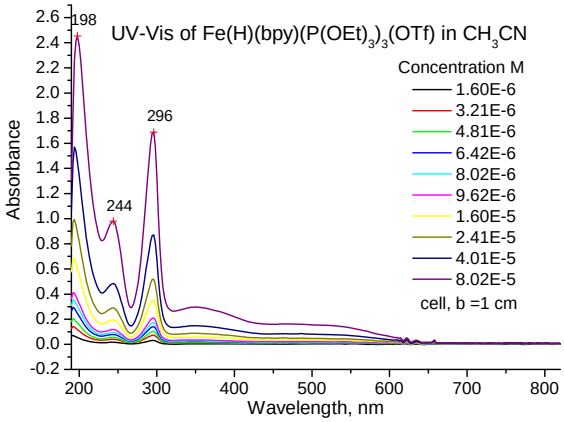

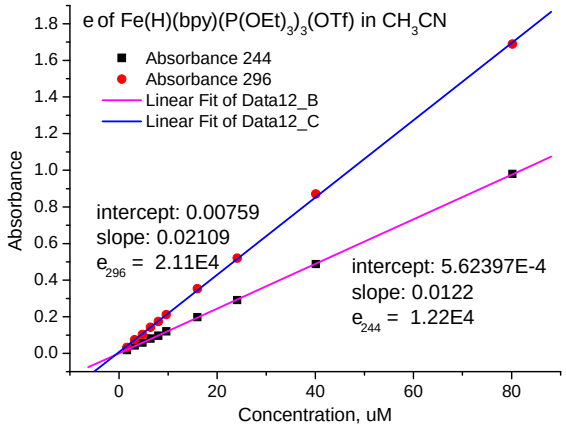

UV-Vis of $Ru(H)(bpy)_2(P(OEt)_3)(PF_6)$ in CH_3CN.

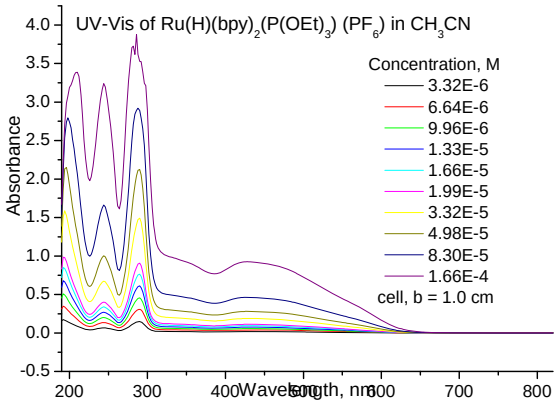

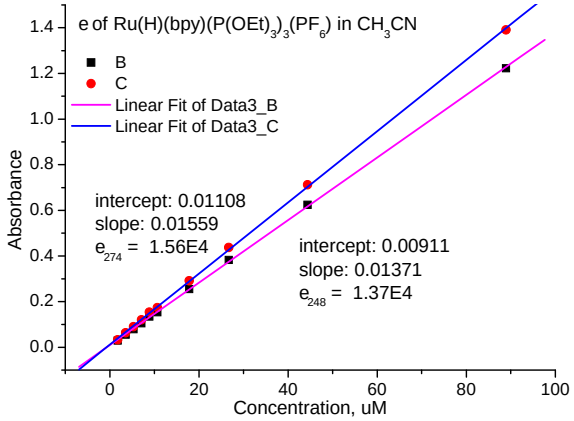

Electrochemical Studies

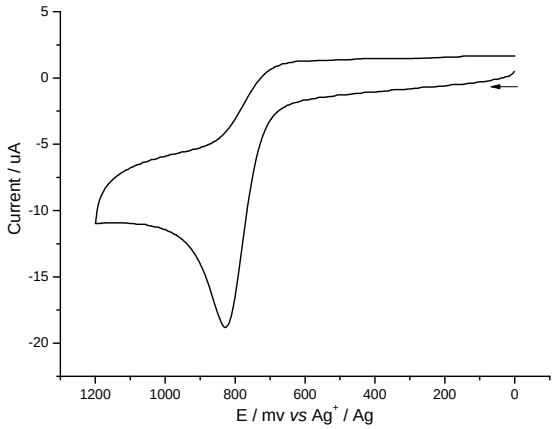

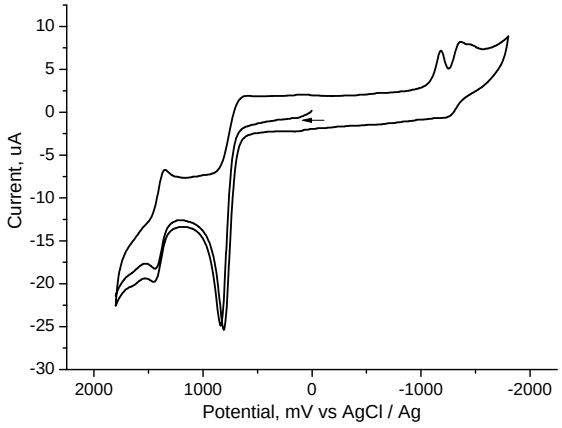

CV of $[Fe(Ph_2PCH_2CH{=}N(C_6H_4)N{=}CHCH_2PPh_2)(CH_3CN)_2][BPh_4]_2$

(Bu_4NPF_6, 0.1 M; CH_3CN, scan rate: 50 mV/s; reference electrode, Ag/AgCl; counter electrode, Pt wire; working electrode, glassy carbon)

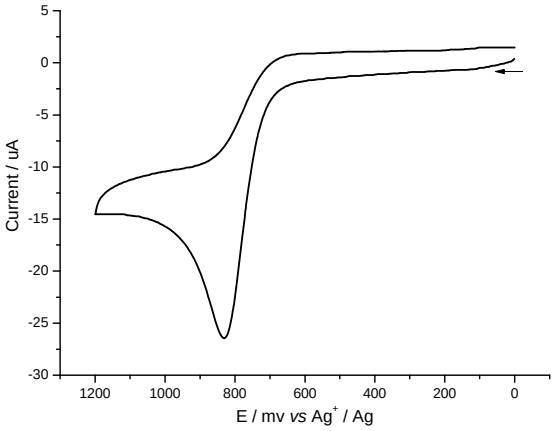

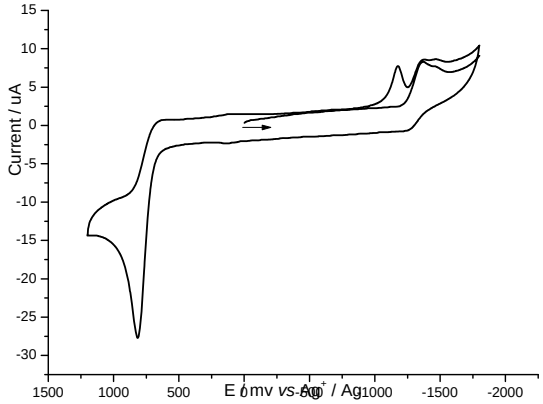

CV of $Fe(Ph_2PCH_2CH=NC_2H_4N=CHCH_2PPh_2)(CH_3CN)_2][BPh_4]_2$

(Bu_4NPF_6, 0.1 M; CH_3CN, scan rate: 50 mV/s; reference electrode, Ag/AgCl; counter electrode, Pt wire; working electrode, glassy carbon)

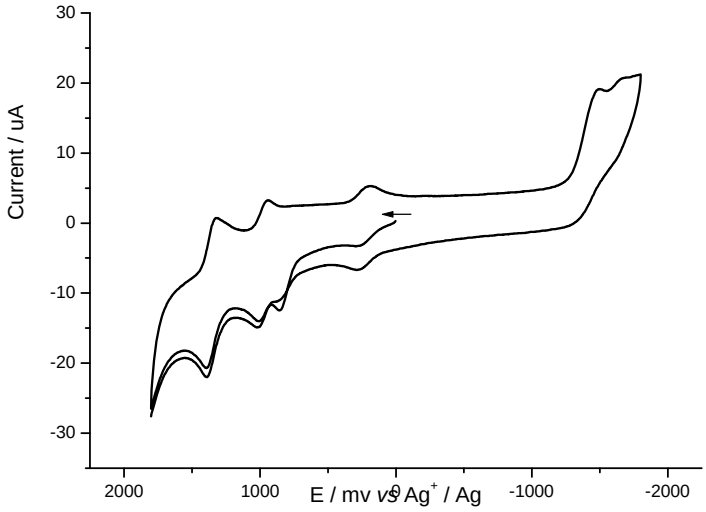

CV of $Fe(Ph_2PCH_2CH=NC_2H_4N=CHCH_2PPh_2)(CH_3CN)_2][BF4]_2$

($Bu4NPF_6$, 0.1 M; CH3CN, scan rate: 50 mV/s; reference electrode, Ag/AgCl; counter electrode, Pt wire; working electrode, glassy carbon)

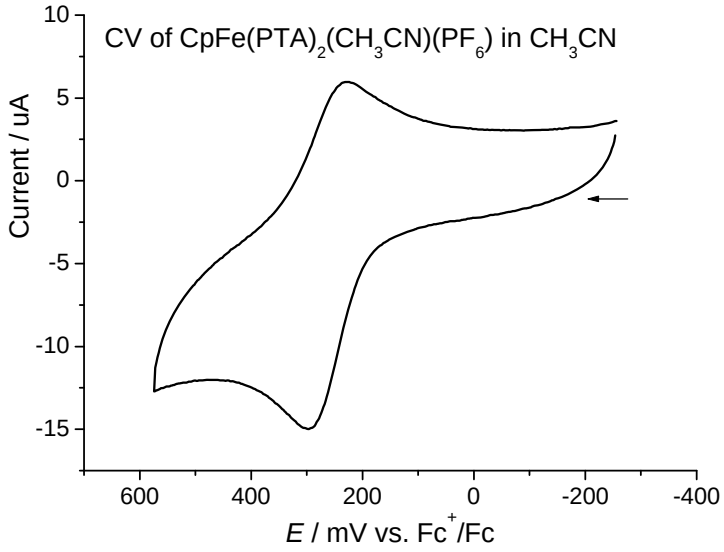

$CpFe(PTA)_2(CH_3CN)(PF_6)$

(Bu_4NPF_6, 0.1 M; CH_3CN, scan rate: 100 mV/s; reference electrode, Ag/AgCl; counter electrode, Pt wire; working electrode, glassy carbon)

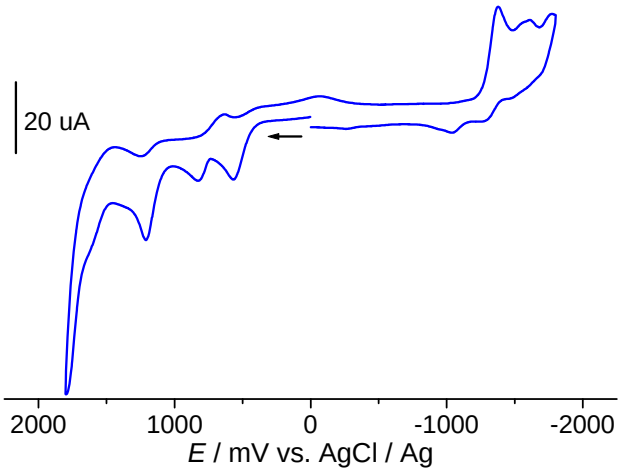

CV of [CpFe(bpy)(CO)]I .

(Bu4NPF6, 0.1 M; CH_3CN, scan rate: 100 mV/s; reference electrode, Ag/AgCl; counter electrode, Pt wire; working electrode, glassy carbon). The first reduction peak is 1374 mV vs. AgCl/Ag; first oxidation is +570 . Numerous other peaks: reduction –1592; oxidation +822, +1209, +1800 mV vs. AgCl/Ag.

Electrochemistry of M(bpy)(P(OEt)$_3$)(H) complexes

Fe(bpy)(P(OEt)$_3$)$_3$(H)(OTf)

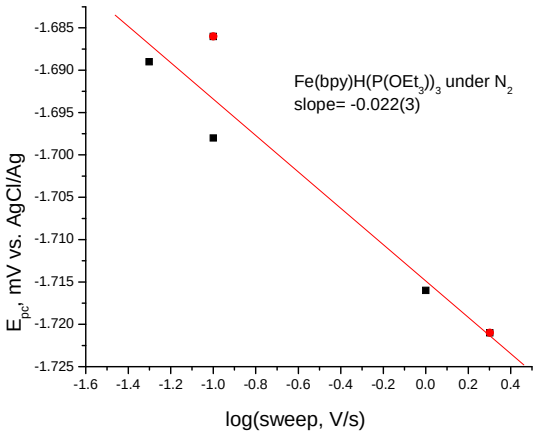

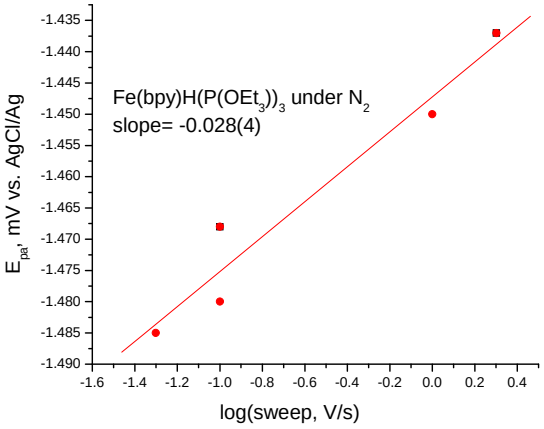

Sweep dependence of cathodic (left) and anodic (right) peak s of Fe(bpy)(P(OEt)$_3$)$_3$(H)(OTf).

The above peak dependence on sweep is consistent with an EC (?EEC) mechanism with k of intermediate magnitude. For n = 2, the slopes should be 59/n; observed values are 0.022 and 0.028. Current ratio <1 with anodic peak tending to disappear at high sweeps.

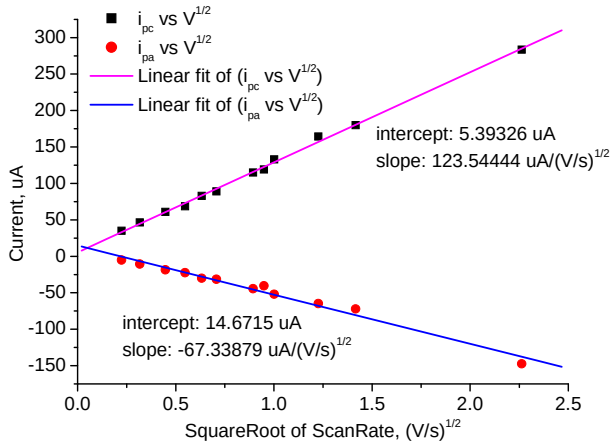

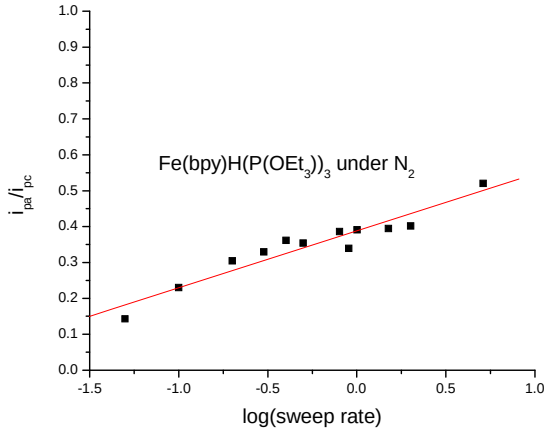

Note that i_{pc} is 3 times greater for the -1.5 V reduction as for i_{pa} for the +0.4 V oxidation; for n = 2 and n= 1 electron processes the ratio should be 2.8.

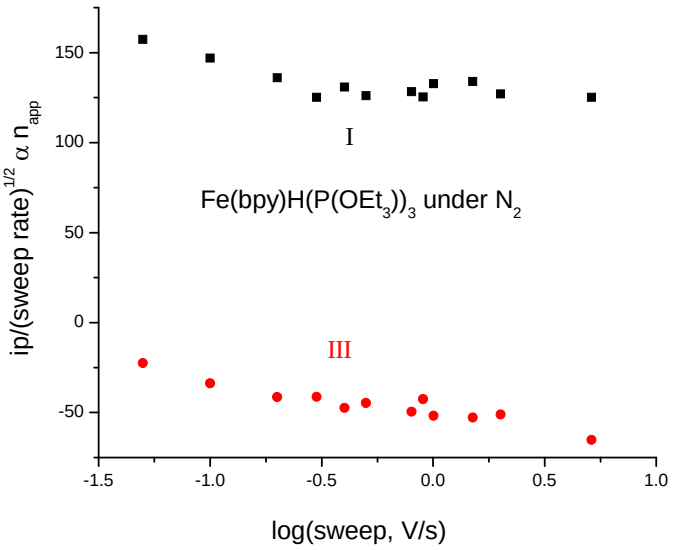

Sweep dependence of current for Fe(bpy)(H)(P(OEt)$_3$)$_3$(OTf) at -1.5 V in CH$_3$CN

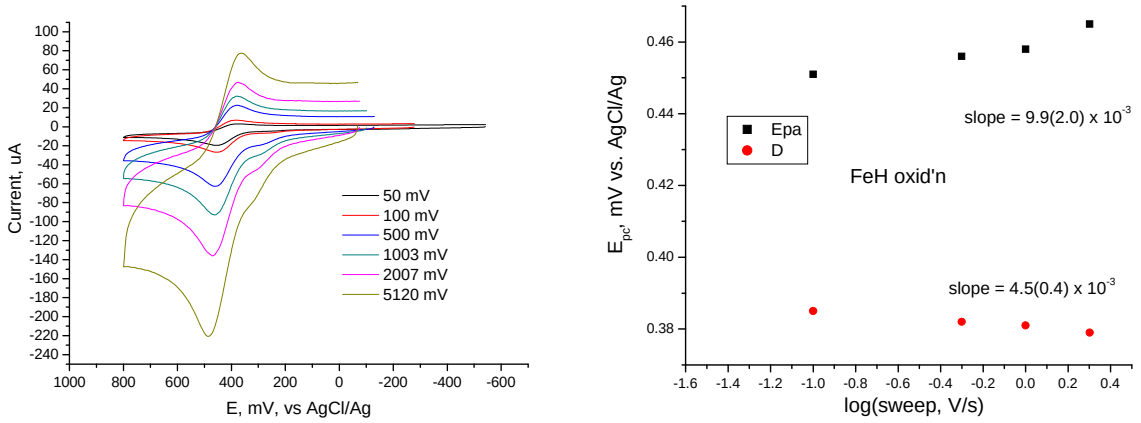

CV of Fe(H)(bpy)(P(OEt)$_3$)$_3$(OTf) 0.58 mM in CH$_3$CN under Argon with different scan rates: 50-5120 mV/s; (Bu$_4$NPF$_6$, 0.1 M; CH$_3$CN, reference electrode, AgCl/Ag (3 M aq. KCl); counter electrode, Pt wire; working electrode, glassy carbon (d = 3 mm) (left). (Right) Dependence of Ep position on sweep rate.

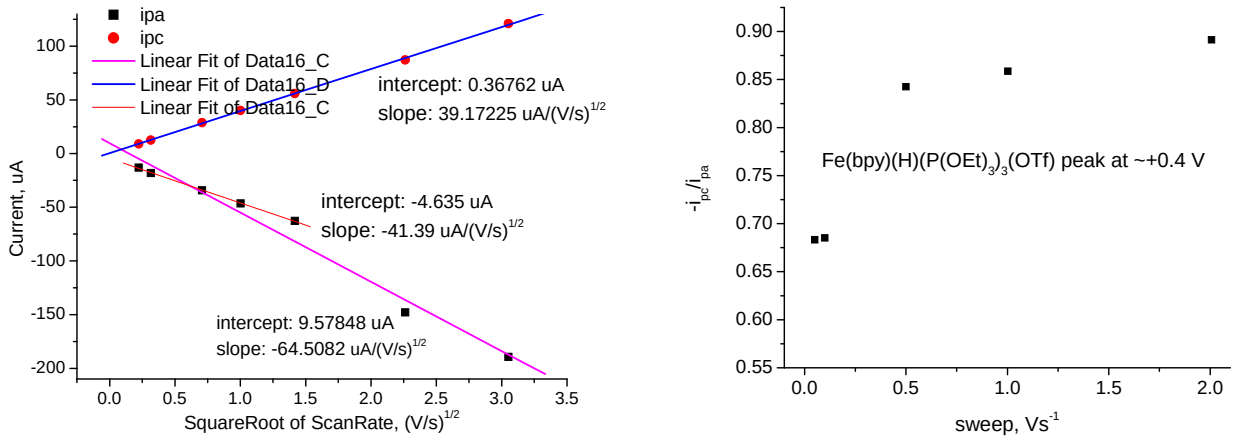

Sweep dependence of current for 0.58 mM Fe(bpy)(H)$(P(OEt)_3)_3$(OTf) at 0.4 V in CH_3CN(left) and dependence of the current ratio on sweep rate (right).

Fe(bpy)$(CH_3CN)(P(OEt)_3)_3(OTf)_2$

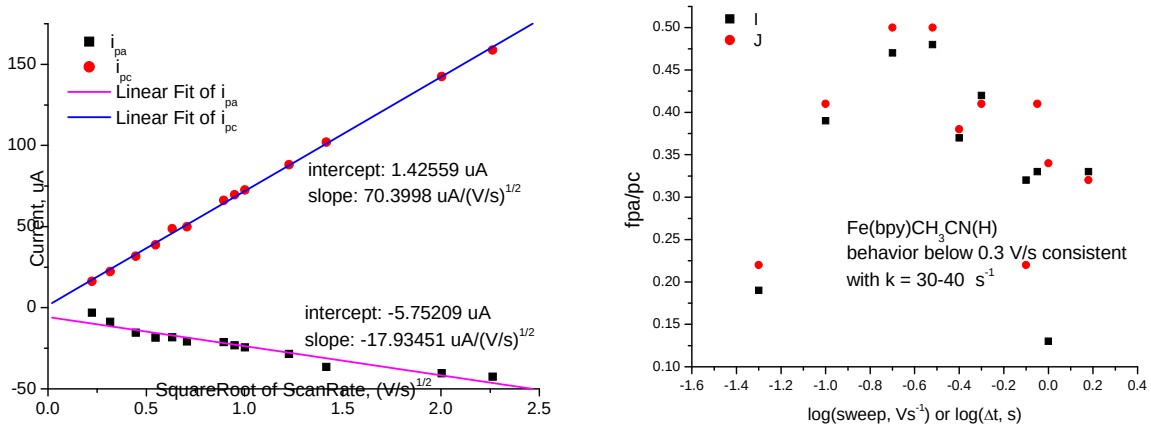

Sweep dependence of current for 0.58 mM Fe(bpy)$(CH_3CN)(P(OEt)_3)_3(OTf)_2$ at -1.1 V in CH_3CN (left) and (right) Dependence of the ration of peaks at -1.1 V on log(sweep) or log(Dt) where Dt is time elapsed from switching time and E0.

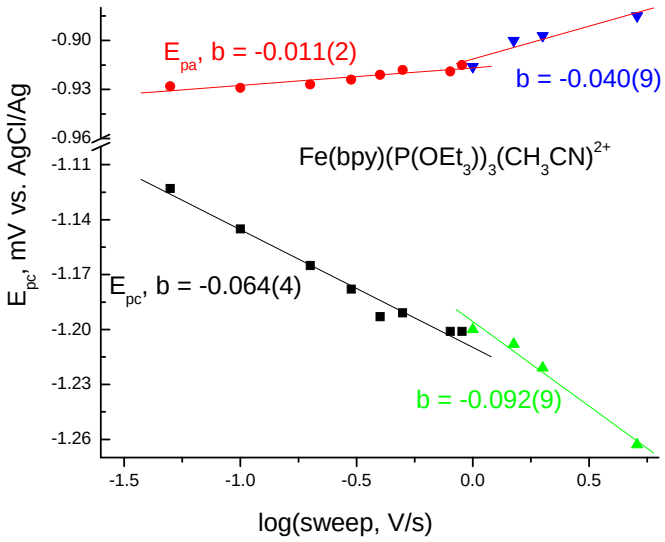

Sweep dependence of peak potentials for ca. -1 V reduction of 0.58 mM $Fe(bpy)(CH_3CN)(P(OEt)_3)_3(OTf)_2$

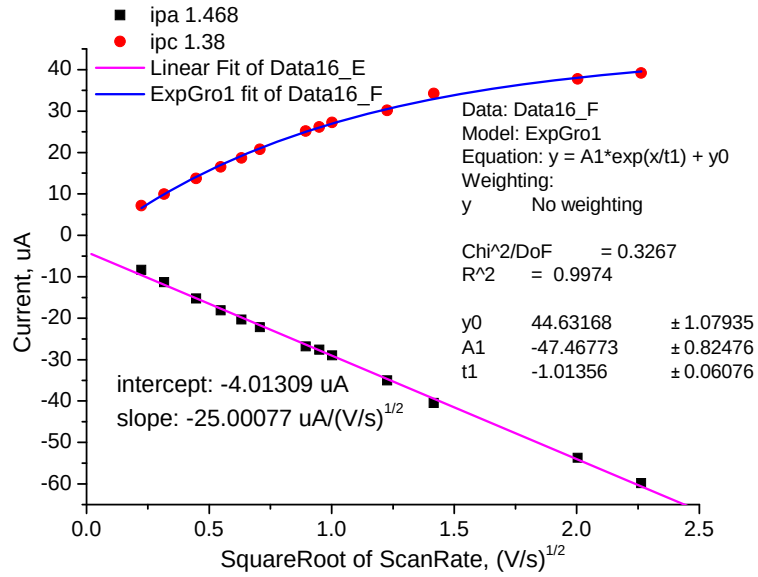

Current Sweep dependence of 0.58 mM $Fe(bpy)(CH_3CN)(P(OEt)_3)_3(OTf)_2$ at 1.4 V in CH_3CN
Compare the -1.1 and +1.4 V slopes, 70 and 25, respectively; 70/25 = 2.8, as expected for 2 and 1 electron changes, respectively.

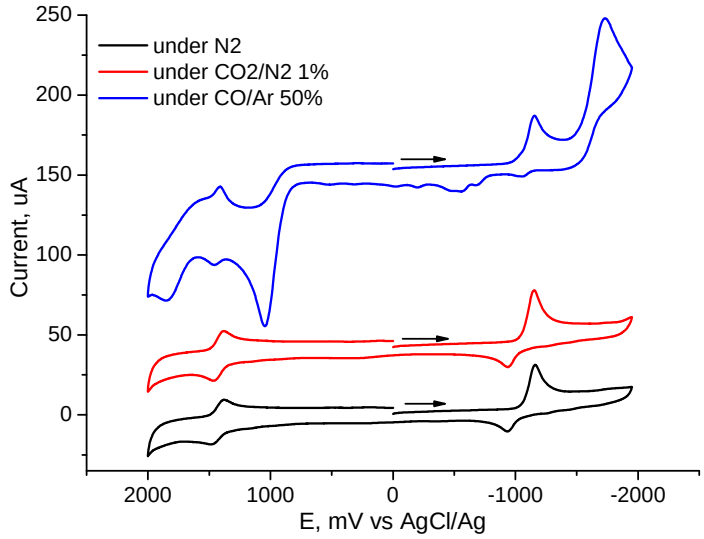

CV of 0.58 mM $Fe(bpy)(CH_3CN)(P(OEt)_3)_3(OTf)_2$ under N_2 (black line), CO_2/N_2 1% (red line) and CO/Ar 50% (blue line) in CH_3CN (Bu_4NPF_6, 0.1 M; CH_3CN, scan rate: 100 mV/s; reference electrode, AgCl/Ag (3 M aq. KCl); counter electrode, Pt wire; working electrode, glassy carbon (d = 3 mm)

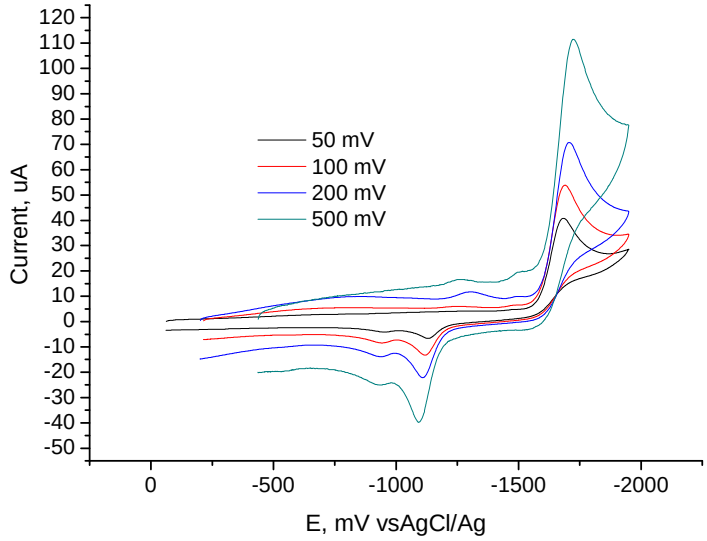

CV of $Fe(H)(bpy)(P(OEt)_3)_3(OTf)$ 0.58 mM in CH_3CN CO_2/N_2 = 1.0% (CO_2, 3 mM in CH_3CN) (Bu_4NPF_6, 0.1 M; CH_3CN, scan rate: 50, 100, 200 and 500 mV/s; reference electrode, AgCl/Ag (3 M aq. KCl); counter electrode, Pt wire; working electrode, glassy carbon (d = 3 mm)

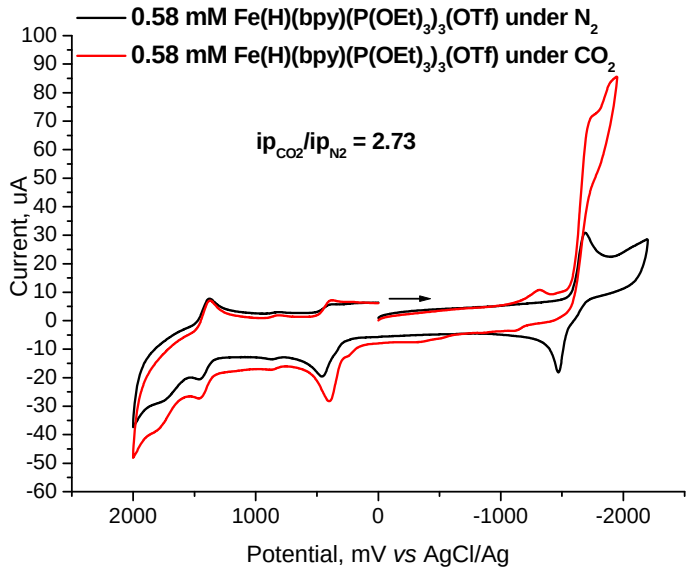

Comparison of currents for reaction of the reduced species $Fe(bpy)(P(OEt_3)_3H^0$ generated at –1.5 V vs. AgCl/Ag without (black) and with CO_2 (red).

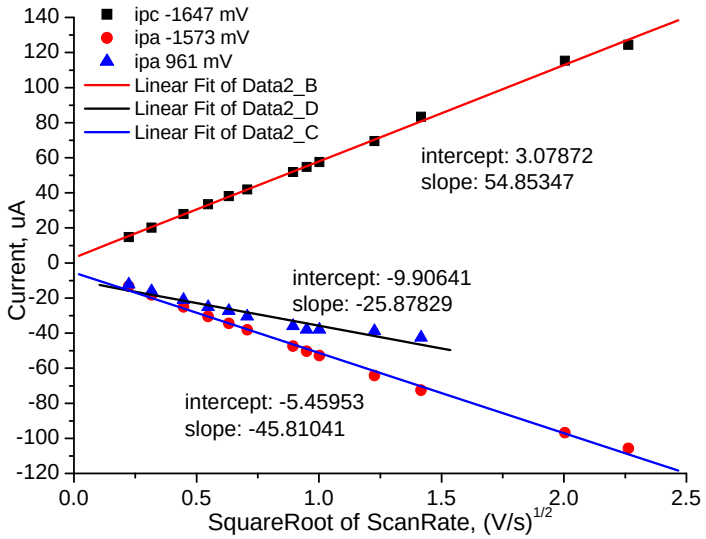

Sweep dependence of 1.0 mM $Ru(bpy)(H)(P(OEt)_3)_3(PF_6)$ under N_2 in CH_3CN at -1.6, -1.5 and 0.9 V in CH_3CN

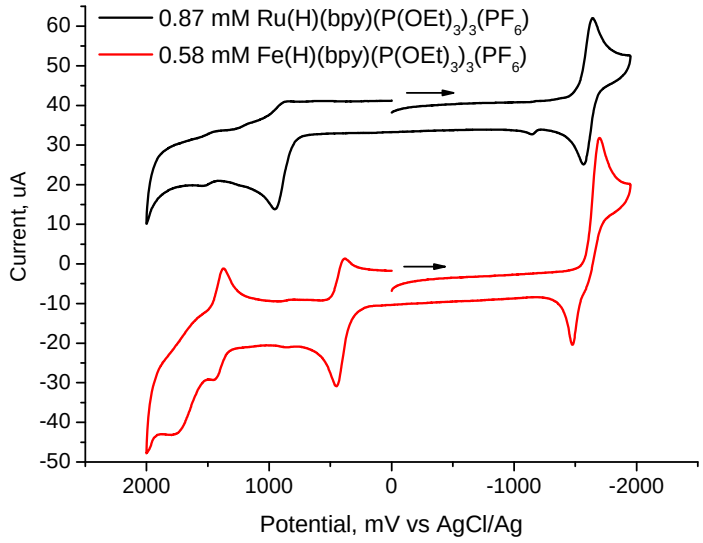

CV of 0.87 mM Ru(bpy)(H)(P(OEt)$_3$)$_3$(PF$_6$) (black) and 0.58 mM Fe(bpy)(H)(P(OEt)$_3$)$_3$(OTf) (red line) under N_2 in CH_3CN (Bu_4NPF_6, 0.1 M; CH_3CN, scan rate: 100 mV/s; reference electrode, AgCl/Ag (3 M aq. KCl); counter electrode, Pt wire; working electrode, glassy carbon (d = 3 mm)

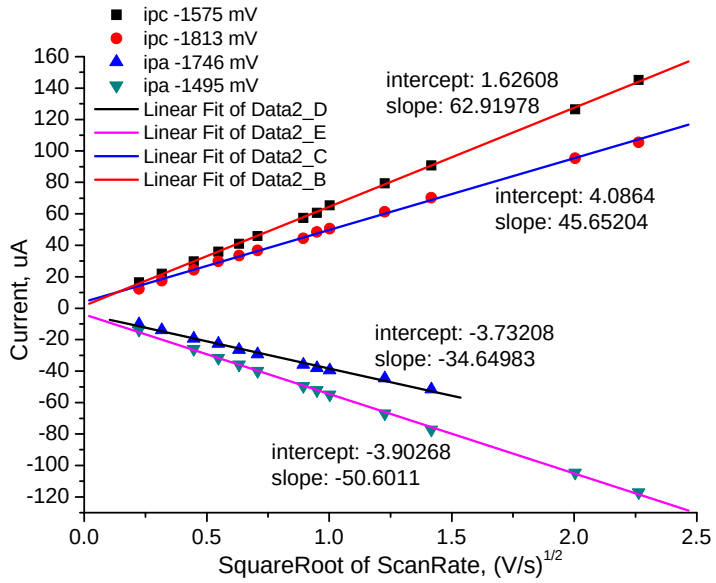

Sweep dependence of 1.0 mM Ru(bpy)$_2$(H)(P(OEt)$_3$)(PF$_6$) under N_2 in CH_3CN at -1.5, -1.8, -1.7 and -1.4 V in CH_3CN

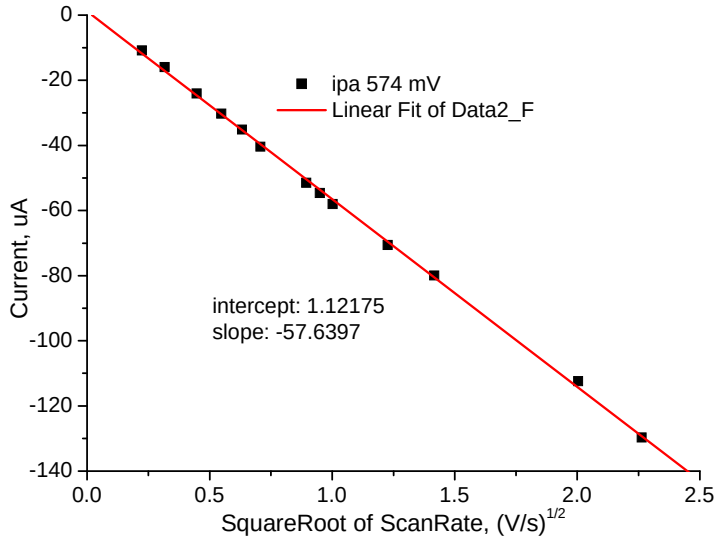

Sweep dependence of 1.0 mM $Ru(bpy)_2(H)(P(OEt)_3)(PF_6)$ under N_2 in CH_3CN at 0.57 V in CH_3CN

Comparisons of redox potentials with other complexes.

M(III)/M(II) couples. It is of interest to compare the iron redox potentials with those found in other systems. Lever and colleagues have parameterized contributions of the various ligands to the metal redox potential according to eq a.[4]

$$E_{redox} = S_M \left(\sum E_L \left(L \right) \right) + I_M \qquad \text{(a)}$$

Data obtained here for M(III)/M(II) couples (see Table S2) are shown as black squares (M = Fe) and red circles (M = Ru) in Figure 14.

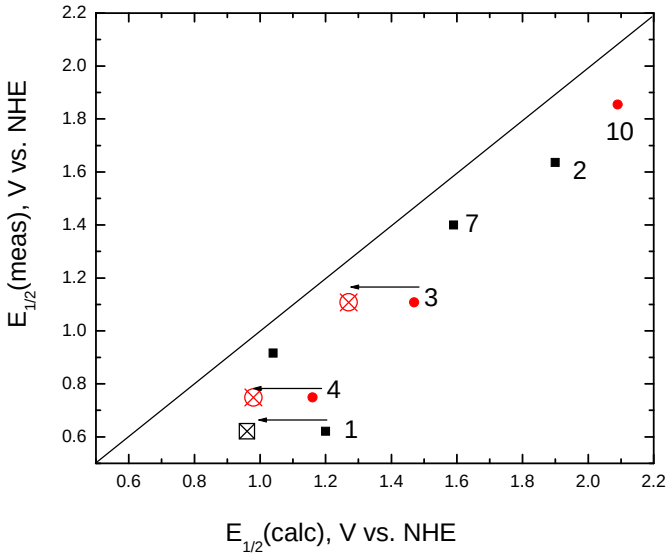

Figure 14. Measured M(III)/M(II) reduction potentials vs. potentials calculated from $E_{redox} = S_m\left(\sum E_L\left(L\right)\right) + I_m$ with S_m = 1.1 , I_m = -0.43 (M = Fe, black squares) and S_m = 0.97, I_m = 0.04 (M = Ru, red circles).[4] The black line is has a slope of 1.0 corresponding to agreement with Lever's work. The numbered points are **1** $Fe(bpy)(P(OEt)_3)_3H^+$, **4** $Ru(bpy)_2(P(OEt)_3)H^+$, **3** $Ru(bpy)(P(OEt)_3)_3H^+$, **7** [CpFe(bpy)(CO)]I, **2** $Fe(bpy)(P(OEt)_3)_3(CH_3CN)^{2+}$, **10** $Ru(bpy)(P(OEt)_3)_3(CH_3CN)^{2+}$. Open squares and circles obtained using $E_L(H^-)$ = -0.5 give behavior more consistent with the other data.

Our values are all lower than predicted, ca. 0.2 V too low for those in best agreement $Fe(bpy)(P(OEt)_3)_3(CH_3CN)^{2+}$, $Ru(bpy)(P(OEt)_3)_3(CH_3CN)^{2+}$, and $CpFe(PTA)_2(CH_3CN)^+$. The hydride complexes lie further below the line based on the Lever value $E_L(H^-)$ = -0.3. The present data suggest a more negative value. Morris has proposed -0.4.[5] As noted by others,[6] the oxidation of the hydride complexes generally occurs at 0.4 to 0.6 V lower potential than the corresponding chloride complex, which suggests the more negative value, $E_L(H^-)$ = -0.6 to -0.8 V vs. NHE. In Figure 10 the open squares and circles were obtained using $E_L(H^-)$ = -0.5.

The oxidation found for $FeL_2(CH_3CN)_2^{2+}$ leads to an evaluation of E_L = +1.14 vs. NHE for the binding to two N and two P sites. This is ~ 100 mV greater than for the four N's in a $(bpy)_2$ unit.

Bpy/Bpy$^-$ Couples. 2,2'-Bipyridine and diimine ligands in general are reducible. Binding to a metal cation raises their reduction potentials.[7] Compare $Rh(bpy)_2^+$, $Ru(bpy)_3^{2+}$, and $Ir(bpy)_3^{3+}$ for which the first bpy reduction lies at -1.43, -1.30,

and -0.83 V, respectively, in CH_3CN or DMF vs. SCE. Dodsworth et al[8] have shown that the reduction potentials of the bound bpy site in metal bipyridine complexes can be varied over 600 mV by changing the ancillary ligands of the complex. The E_L values used for the ancillary ligands are the same as those that correlate metal-centered reduction processes,[4] but the slopes S_L (S_M near unity for 3+/2+ couples of Fe, Ru, and Os) are smaller than for the metal-centered processes. With use of literature data bpy-reduction potentials for the Ru complexes can be estimated and those for Fe may be assumed to be the same. Data obtained here (black squares) are compared with those which Dodsworth reported for bpy reduction in Figure 15. The slope of the correlation was 0.25. Only **7**, $CpFe(bpy)(CO)^+$ is clearly consistent with the literature data. $Fe(bpy)(P(OEt)_3)_3(CH_3CN)^{2+}$ (2), a two-electron reduction, lies too high, suggesting that bpy is not the reduction site. Outliers **4**, **1**, and **3** are all hydrides and lie too low. For the two M = Ru complexes classically shaped reversible one-electron reductions characteristic of ligand reduction and spectroscopic signatures of the reduced ligand (vide infra) were observed, confirming bpy-reduction and thus -suggesting again that E_L for hydride should be more negative than -0.3.

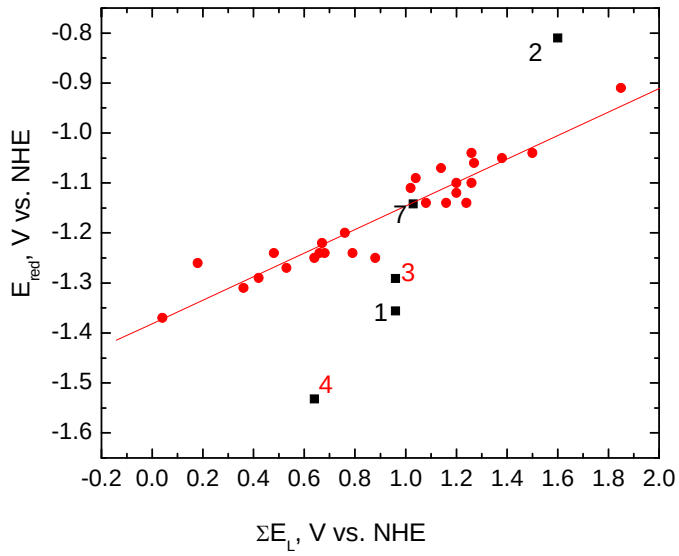

Figure 15. Potentials for reduction of bound polypyridyl ligands as a function of the sum of E_L values for the other ligands, $E_{red} = S_L \sum E_L(L) + I_L$.[8] The numbered points are **4**, $Ru(bpy)_2(P(OEt)_3)H^+$, **1** $Fe(bpy)(P(OEt)_3)_3H^+$, **3** $Ru(bpy)(P(OEt)_3)_3H^+$, **7** [CpFe(bpy)(CO)]I, **2** $Fe(bpy)(P(OEt)_3)_3(CH_3CN)^{2+}$. The line is a least-squares fit with slope 0.24 and intercept -1.38.

Fe(II)/Fe(I) Couples. We turn next to consider the $Fe^{II/I}$ and $Fe^{I/0}$ couples (see Tables S3 and S4). As for the $M^{III/II}$ couples, we use the E_L data set of Lever along with the results of Lu et al.[9] to estimate potentials for reduction involving the

Fe(II)/(I) couple. Figure 16 compares observed and calculated values for the original ferrocene-type data set, for reduction of $Fe(dppe)_2(H)L^{+}$[10] (= py, N_2, etc.) and **1** $Fe(bpy)(P(OEt)_3)_3H^+$, **7** [CpFe(bpy)(CO)]I, **2** $Fe(bpy)(P(OEt)_3)_3(CH_3CN)^{2+}$. The latter points seem to correlate well with those of Pilloni[10] for the cationic hydride complexes $Fe(dppe)_2(H)L^+$ and all appear to lie on a line parallel to the sandwich complex data with a somewhat more positive intercept than for the sandwich complexes. Thus these considerations are consistent with the metal as the first reduction site for **1** $Fe(bpy)(P(OEt)_3)_3H^+$ and **2** $Fe(bpy)(P(OEt)_3)_3(CH_3CN)^{2+}$ i.e. the $Fe^{II}(bpy)/Fe^{I}(bpy)$ couple is the electrochemically active one here. A pentaphosphine chloroiron(II) complex is reduced to Fe(0) at -1.65 V vs. AgCl/Ag.[11]

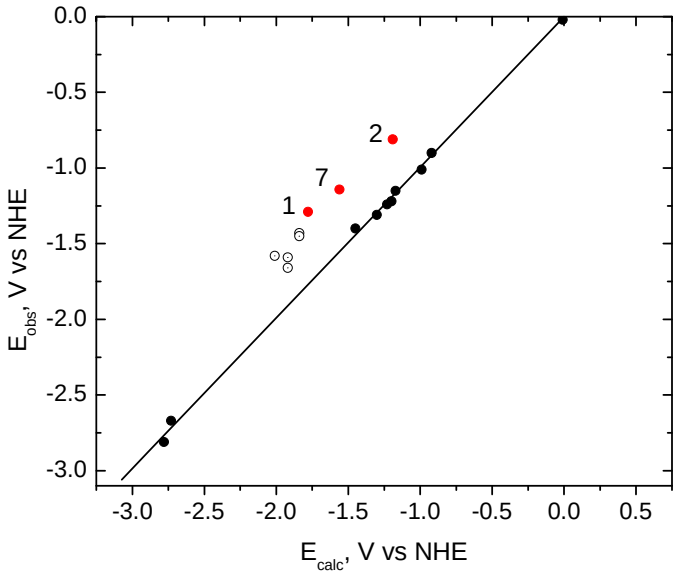

Figure 16. Observed vs. calculated Fe(II/I) reduction potentials for reduction of sandwich complexes of the ferrocene type[9] (solid black circle, black line), $Fe(dppe)_2HL^+$ (Pilloni et al.,[10] open circles) and Fe(II) complexes studied here (red circles).**1** $Fe(bpy)(P(OEt)_3)_3H^+$, **7** [CpFe(bpy)(CO)]I, and **2** $Fe(bpy)(P(OEt)_3)_3(CH_3CN)^{2+}$. See Table S2.

Literature Electrochemical Data

Table S2.Comparison of M(III)/(II) Metal-centered reduction potentials and ΣE_L values[4]

Complex	E_{av}, mV vs. SHE	ΣE_L, V	E_{calc}
[CpFe(bpy)(CO)]I	(+0.77)	1.548	1.27
$CpFe(PTA)_2(CH_3CN)(PF_6)$	+0.91	1.34	1.04

$Fe(bpy)(P(OEt)_3)_3H^+$	+0.62	1.478	1.20
$Ru(bpy)(P(OEt)_3)_3H^+$	+1,10	1.478	1.47
$Ru(bpy)_2(P(OEt)_3)H^+$	(+0.75)	1.156	1.16
$Fe(bpy)(P(OEt)_3)_3(CH_3CN)^{2+}$	+1.63	2.118	1.90
$Ru(bpy)_2(P(OEt)_3)(CH_3CN)^{2+}$	+1.86	2.118	2.09

Table S3. The Fe(II)/(I) Potential

All FeII/I

Pilloni, G.; Zotti, G.; Mulazzani, Q. G.; Fuochi, P. G. Journal of Electroanalytical Chemistry 1982, 137, 89-102.

Pilloni et al — DPE = 1,2-bis(diphenylphosphineoethane) — EL = 0.36 — reduction of cation

Fe(H)L(DPE)2

L	E vs Ag	E_L Lever	$sumE_L$	calc E vs NHE	Eobs vs NHE
N2	-1.97	0.68	1.82	-1.58	-1.38
Py	-2.17	0.25	1.39	-2.01	-1.58
C6H5CN	-2.18	0.34	1.48	-1.92	-1.59
CH3CN	-2.25	0.34	1.48	-1.92	-1.66
P(OCH3)3	-2.02	0.42	1.56	-1.84	-1.43
P(OEt3)3	-2.04	0.42	1.56	-1.84	-1.45
CO	-1.98	0.99	2.13	-1.27	-1.39

Lever gives IM = 3.4

	Lu,Strelet Lever		
	sumEL	Ecalc	Eobs
$FeCp_{2}$-	0.66	-2.73	-2.67
	0.61	-2.78	-2.81
	1.92	-1.45	-1.4
	2.13	-1.23	-1.24
	2.16	-1.2	-1.22
	2.19	-1.17	-1.15
	2.37	-0.99	-1.01
	2.44	-0.92	-0.9
	2.06	-1.3	-1.31
	3.46	0.16	0.18
$Fe(HMB)_2$-	3.32	-0.01	-0.02

Lu, S. X.; Strelets, V. V.; Ryan, M. F.; Pietro, W. J.; Lever, A. B. P. *Inorg. Chem.* **1996**, *35*, 1013-1023.

Table S4. The Fe(I)/(0) Potential

Eobs values from Abdelaziz, A. S., A. S. Baranski, et al. (1988). Inorganica Chimica Acta 147(1): 77-85.

CpFeL			vs AgNO3			vs NHE	
L	EL	sumEL	II/I	I/0	dif	II/I	I/0

Nme2	1.69	2.02	-1.95	-2.67	0.72	-1.36	-2.08
Ome	1.81	2.14	-1.83	-2.6	0.77	-1.24	-2.01
t-Bu	1.82	2.15	-1.82	-2.46	0.64	-1.23	-1.87
Et	1.77	2.1	-1.81	-2.62	0.81	-1.22	-2.03
Oph	1.9	2.23	-1.74	-2.49	0.75	-1.15	-1.9
Me	1.79	2.12	-1.71	-2.47	0.76	-1.12	-1.88
CH2Ph	1.93	2.26	-1.7	-2.37	0.67	-1.11	-1.78
Ph	1.96	2.29	-1.66	-2.25	0.59	-1.07	-1.66
Cl	2.03	2.36	-1.6	-2.19	0.59	-1.01	-1.6
CO2Me	2.11	2.44	-1.52	-2.12	0.6	-0.93	-1.53
COPh	2.17	2.5	-1.46	-2.19	0.73	-0.87	-1.6
CN	2.18	2.51	-1.45	-2.12	0.67	-0.86	-1.53
NO2	2.58	2.91	-1.04	-1.49	0.45	-0.45	-0.9
CpFeL	0.33	0.66					
Cp*	0.06						

EL values from Lu, S. X.; Strelets, V. V.; Ryan, M. F.; Pietro, W. J.; Lever, A. B. P. *Inorg. Chem.* **1996**, *35*, 1013-1023.

Table S6. Potentials of Os(II) and Ru(II) hydride complexes.

E_L hydrides Os data from Sullivan[12]

		$\Sigma^5 E_L$, V vs. NHE	Cl	H vs NHE	
1	$[Ru(bpy)_2(CO)X^+$	2.03	1.74	1.38	
2	$[Os(bpy)_2(CO)X^+$	2.03		1.12	
3	$[Os(phen)_2(CO)H]^+$	2.03		1.14	
4	$[Os(phen)(dppb)(PPh_3)H^+$	1.81		1.07	
5	$[Os(phen)(dppy)(PPh_3)H]^+$	1.89		1.04	
6	$[Os(phen)(dppy)(PEt_3)H]^+$	1.84		0.98	
7	trans-$[Os(bpy)(PPh_3)_2(CO)H]^+$	2.29		1.78	
8	trans-$[Os(bpym)(PPh_3)_2(CO)H]^+$	2.39		1.79	
9	trans-$[Os(bpyz)(PPh_3)_2(CO)H]^+$	2.37		1.78	
10	*trans*-[Os(3,4,7,8-Me_4phen)(PPh,)(CO)H]$^+$			1.46	
11	$[Os(phen)(dppb)(CO)Cl]^+$	2,41	1.66		
12	$[Os(phen)(dppy)(CO)Cl]^+$	2.49	1.78		
13	trans-$[Os(phen)(PMe_2Ph)_2(CO)Cl]^+$	2.17	1.52		
14	*trans*-$[Os(phen)(PMe_3)_2(CO)Cl]^+$	2.17	1.49		
15	*trans*-$[Os(phen)(PMe_2Ph)(CO)Cl]^+$	1.89	1.65		
16	*trans*-$[Os(phen)(PPh_3)_2(CO)Cl]^+$	1.9	1.74		
17	$[Os(phen)(dppy)(PMe_2Ph)Cl^+$	1.82	1.04		

18	$[Ru(bpy)_2(CO)Cl]^+$	2.03	1.74		
19	$[Os(bpy)_2(CO)Cl]^+$	2.03	1.42		
1	$[Ru(bpy)_2(CO)X]^+$	2.03	1.74	1.27[13]	
	$Ru(bpy)_2(PPh_3)H^+$	1.43		0.81[13]	
	$Ru(bpy)_2(AsPh_3)H^+$	1.42		0.81[13]	
	$Ru(bpy)(P(OEt)_3)_3H^+$	1.78		+0.95	
	$Ru(bpy)_2(P(OEt)_3)H^+$	1.56		+0.55	
	$Ru(bpy)(terpy)H^+$	1.27		+0.43[14]	
	CpRu(dtfpe)H	1.27		0.77	
	CpRuH(dppe)	1.05		0.51	
	$CpRuH(PPh_3)_2$	1.11		0.4	
	CpRuH(dape)	0.99		0.38	
	Cp*RuH(dppm)	0.92		0.35	
	Cp*RuH(dppp)	0.76		0.16	
	$Cp^*RuH(PPh_3)_2$	0.84		0.14	
	$Cp^*RuH(PMePh_2)_2$	0.8		0.11	
	$Cp^*RuH(PMe_2Ph)_2$	0.72		0.03	
	$Cp^*RuH(PMe_3)_2$	0.62		-0.02	
	$CpRuH(PMe_3)(CO)$	1.62		1.02[15]	
	Cp*RuH(dppm)	0.88		0.35	
	Cp*RuH(dppp)	0.72		0.16	
	$Cp^*RuH(PPh_3)_2$	0.8		0.14	
	$Cp^*RuH(PMePh_2)_2$	0.76		0.11	
	$Cp^*RuH(PMe_2Ph)_2$	0.68		0.03	
	$Cp^*RuH(PMe_3)_2$	0.62		-0.02	
	$CpRuH(PMe_3)(CO)$	1.62		1.02[15]	

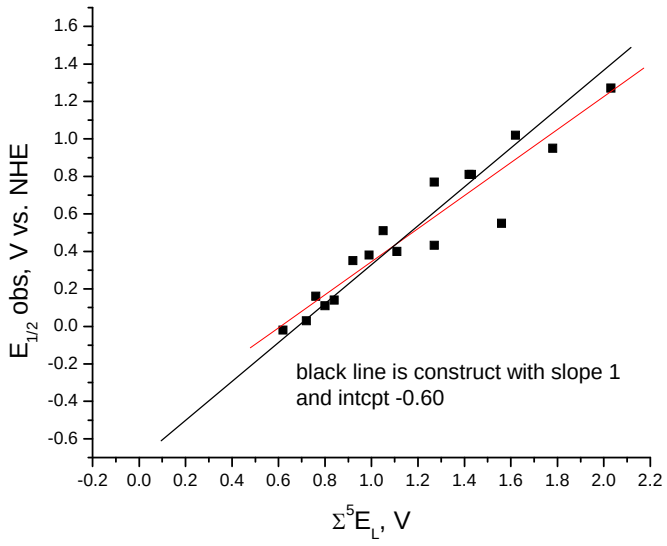

Reactivity Studies

Dependence of cathodic current on acetic acid concentration for $Fe(bpy)(P(OEt)_3)_3(CH_3CN)(OTf)_2$.

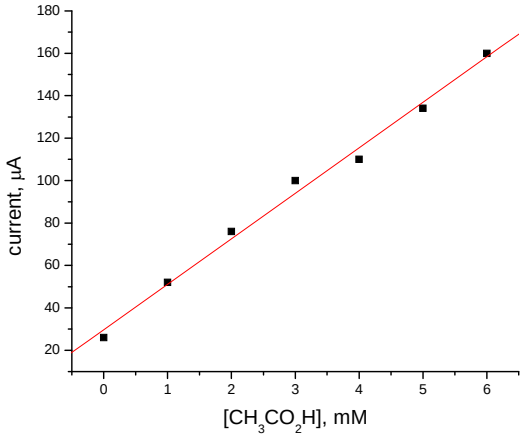

$Ru(H)(bpy)_2(P(OEt)_3)(PF_6)$ + CO_2

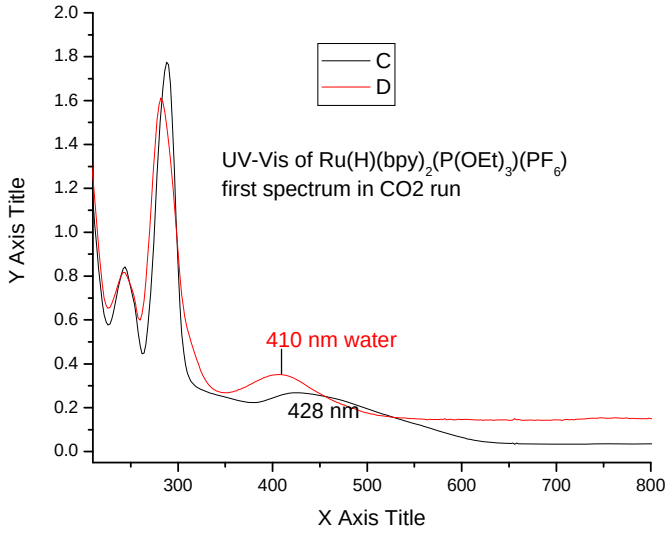

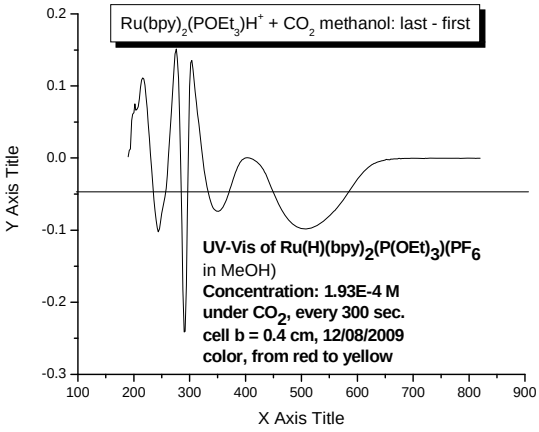

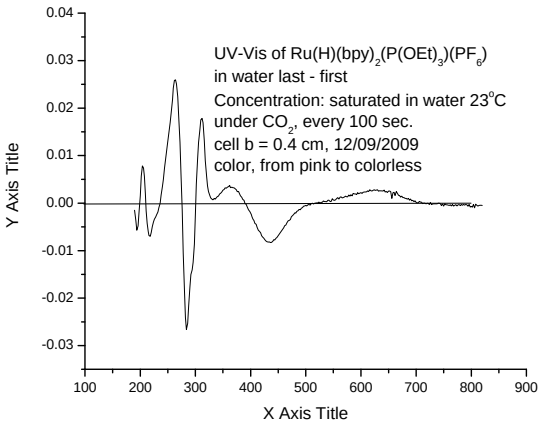

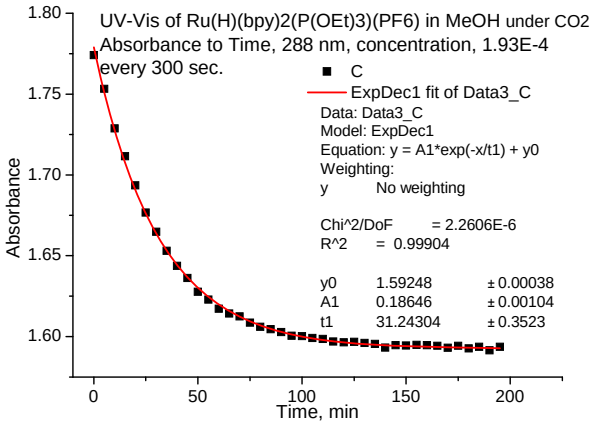

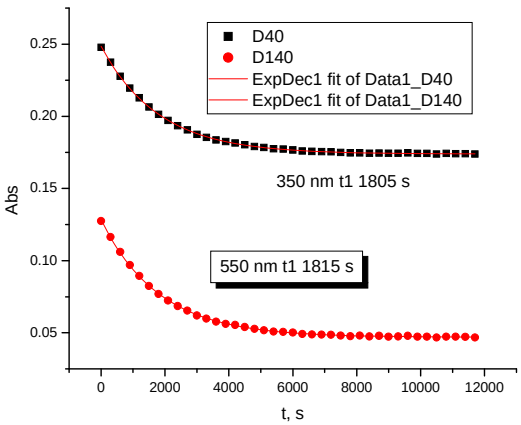

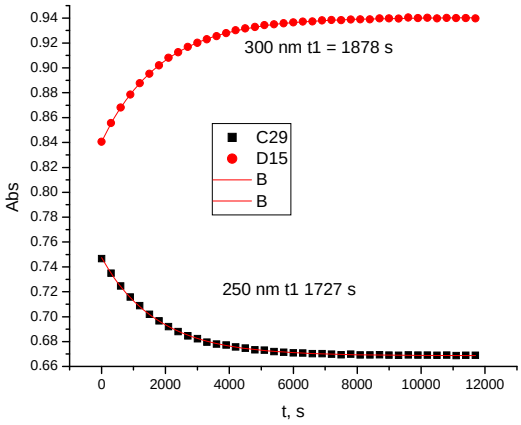

UV-Vis of $Ru(H)(bpy)_2(P(OEt)_3)(PF_6)$ in MeOH under CO_2, Absorbance vs. Time, λ= 288 nm, the first order exponential decay, (Concentration: 1.93E-4 M), every 300 sec., cell b = 0.4 cm, color, from red to yellow. Averaging over the five wavelengths gives t1 = 1818 s, kobs = 5.5 x 10-4 s-1, and dividing by the CO_2 solubility in MeOH, 0.14 M/atm, estimate second order rate constant of 3.9 x 10^{-3} M^{-1} s^{-1}. That for Ru(terpy)(bpy)H+ is 1200 times greater.[16]

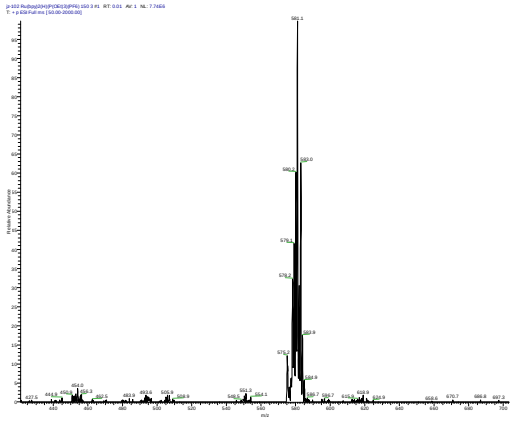

Before bubbling CO_2 in the UV-Vis experiment.
M^+ $[Ru(bpy)_2(H)(P(OEt)_3)]^+$ m/e = 581.1
$Ru(bpy)_2(H)(P(OEt)_3)(PF_6)$ Conditions: Sheath Gas Flow Rate 5, Auxiliary Gas Flow Rate 0, Spray Voltage 3.0 KV, Capillary Temperature 150, Capillary Voltage 24, Tube Lens Offset Voltage 35

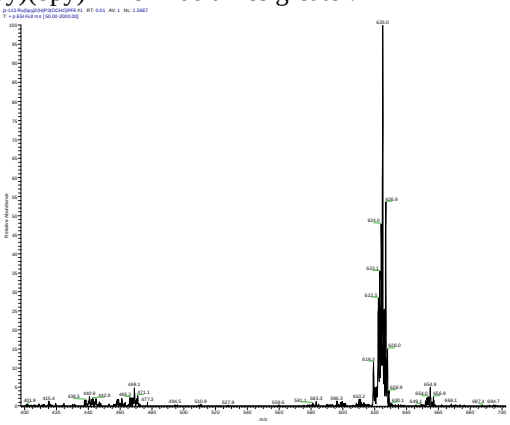

After bubbling CO_2 in the UV-Vis experiment.
M^+ $[Ru(bpy)_2(OCHO)(P(OEt)_3)]^+$ m/e = 625.0
$Ru(bpy)_2(H)(P(OEt)_3)(PF_6)$ + CO_2 150 3.RAW, Conditions: Sheath Gas Flow Rate 5, Auxiliary Gas Flow Rate 0, Spray Voltage 3.0 KV, Capillary Temperature 150, Capillary Voltage 24, Tube Lens Offset Voltage 35

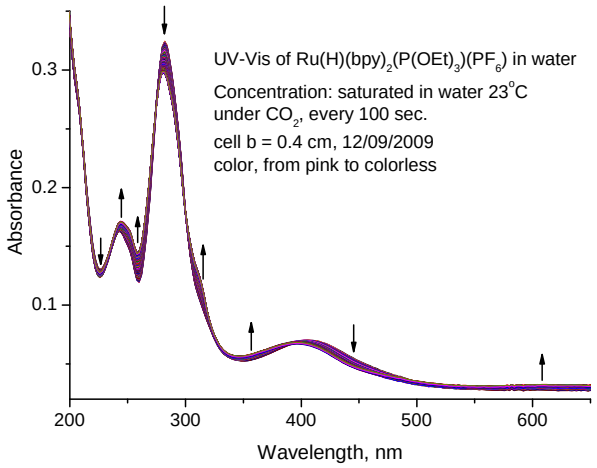

UV-Vis of saturated $Ru(H)(bpy)_2(P(OEt)_3)(PF_6)$ in water under CO_2, every 100 sec., cell b = 0.4 cm, color, from pink to colorless

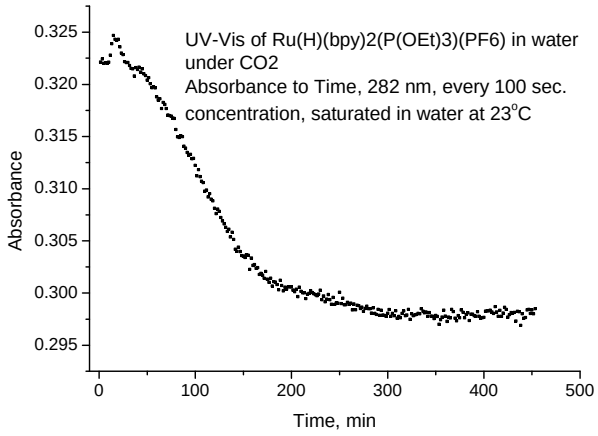

UV-Vis of saturated $Ru(H)(bpy)_2(P(OEt)_3)(PF_6)$ in water under CO_2, Absorbance vs. Time, every 100 sec., cell b = 0.4 cm, color, from pink to colorless

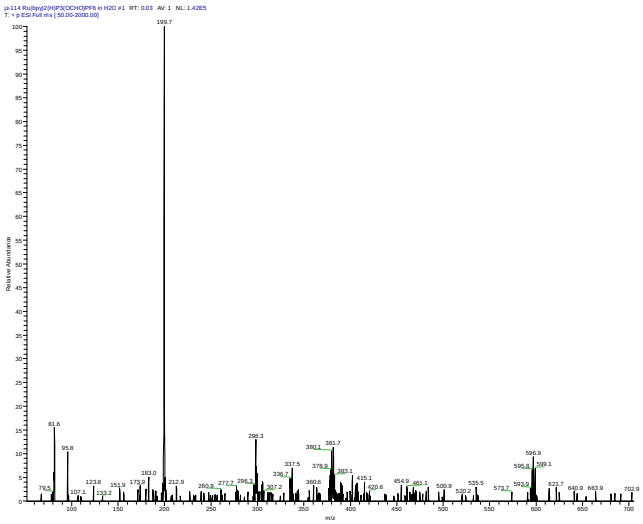

After bubbling CO_2 in the UV-Vis experiment.
M+ $[Ru(bpy)_2(OH)(P(OEt)_3)]$ m/e = 596.9
M+/2 m/e = 298.3
M+/3 m/e = 199.7
$Ru(bpy)_2(H)(P(OEt)_3)(PF_6)$ + CO_2 in water, 150 3.RAW
Conditions: Sheath Gas Flow Rate 5, Auxiliary Gas Flow Rate 0, Spray Voltage 3.0 KV, Capillary Temperature 150, Capillary Voltage 24, Tube Lens Offset Voltage 35

(1) Treichel, P. M.; Shubkin, R. L.; Barnett, K. W.; Reichard, D., *Inorg. Chem.* **1966,** 5, 1177-&.
(2) Darensbourg, D. J.; Phelps, A. L.; Adams, M. J.; Yarbrough, J. C., *J. Organomet. Chem.* **2003,** 666, 49-53.
(3) Frost, B. J.; Mebi, C. A., *Organometallics* **2004,** 23, 5317-5323.
(4) Lever, A. B. P., *Inorg. Chem.* **1990,** 29, 1271-1285.
(5) Morris, R. H., *Inorg. Chem.* **1992,** 31, 1471-1478.

(6) Shaw, A. P.; Norton, J. R.; Buccella, D.; Sites, L. A.; Kleinbach, S. S.; Jarem, D. A.; Bocage, K. M.; Nataro, C., *Organometallics* **2009,** 28, 3804-3814.
(7) Creutz, C., *Comments Inorg. Chem.* **1982,** 1, 293-311.
(8) Dodsworth, E. S.; Vlcek, A. A.; Lever, A. B. P., *Inorg. Chem.* **1994,** 33, 1045-1049.
(9) Lu, S. X.; Strelets, V. V.; Ryan, M. F.; Pietro, W. J.; Lever, A. B. P., *Inorg. Chem.* **1996,** 35, 1013-1023.
(10) Pilloni, G.; Zotti, G.; Mulazzani, Q. G.; Fuochi, P. G., *J. Electroanal. Chem.* **1982,** 137, 89-102.
(11) Thoreson, K. A.; Follett, A. D.; McNeill, K., *Inorg. Chem.* **2010,** 49, 3942-3949.
(12) Sullivan, B. P.; Caspar, J. V.; Meyer, T. J.; Johnson, S., *Organometallics* **1984,** 3, 1241-1251.
(13) Kelly, J. M.; Vos, J. G., *J. Chem. Soc., Dalton Trans.*, **1986,** 1045-1048.
(14) Konno, H.; Ishii, Y.; Sakamoto, K.; Ishitani, O., *Polyhedron* **2002,** 21, 61-68.
(15) Ryan, O. B.; Tilset, M.; Parker, V. D., *Organometallics* **1991,** 10, 298-304.
(16) Konno, H.; Kobayashi, A.; Sakamoto, K.; Fagalde, F.; Katz, N. E.; Saitoh, H.; Ishitani, O., *Inorg. Chim. Acta* **2000,** 299, 155-163.